



ΔΙΕΡΓΑΣΙΕΣ ΔΙΑΧΩΡΙΣΜΟΥ

Μάθημα 10ο

Ακαδημαϊκό έτος 2017-2018

Separation Processes

Quantitative description of combined mechanisms: **Volume diffusion & Surface integration**

Combination of mechanisms:

Driving force: $c - c'$

$$\dot{r}_D = k_d (c - c')$$

Overall rate is:

For crystals $< 5\mu$

$$k_d = \frac{DV_m}{r}$$

For larger sizes:

$$k_d = \frac{DV_m}{\delta}$$

The driving force for the attachment of growth units to the surface is $c' - c_{eq}$ and the rate of crystallization is:

$$\dot{r} = k_g (c' - c_{eq})^g$$

Elimination of the unknown concentration c' gives:

$$\dot{r} = k_g \left[(c - c_{eq}) - \frac{\dot{r}}{k_d} \right]^g$$

rearranging

$$\Psi_I = (1 - \Psi_I h_1)^g$$

$$\Psi_D = h_1 (1 - \Psi_D)^g$$

$$h_1 = \frac{k_g (c - c_{eq})^{g-1}}{k_d}$$

Separation Processes

The significance of diffusion may be assessed from the calculation of the integration coefficient:

$\Psi_I =$ (crystal growth rate at the interface conditions) / (rate of crystallization if the surface were exposed to bulk solution conditions)

$=$ (actual crystal growth rate) / (rate with rds surface diffusion)

$$= \frac{\dot{r}}{\dot{r}_1}$$

If the rate determining step were diffusion the respective coefficient should be:

$\Psi_D =$ (rate) / (rate with rds bulk diffusion)

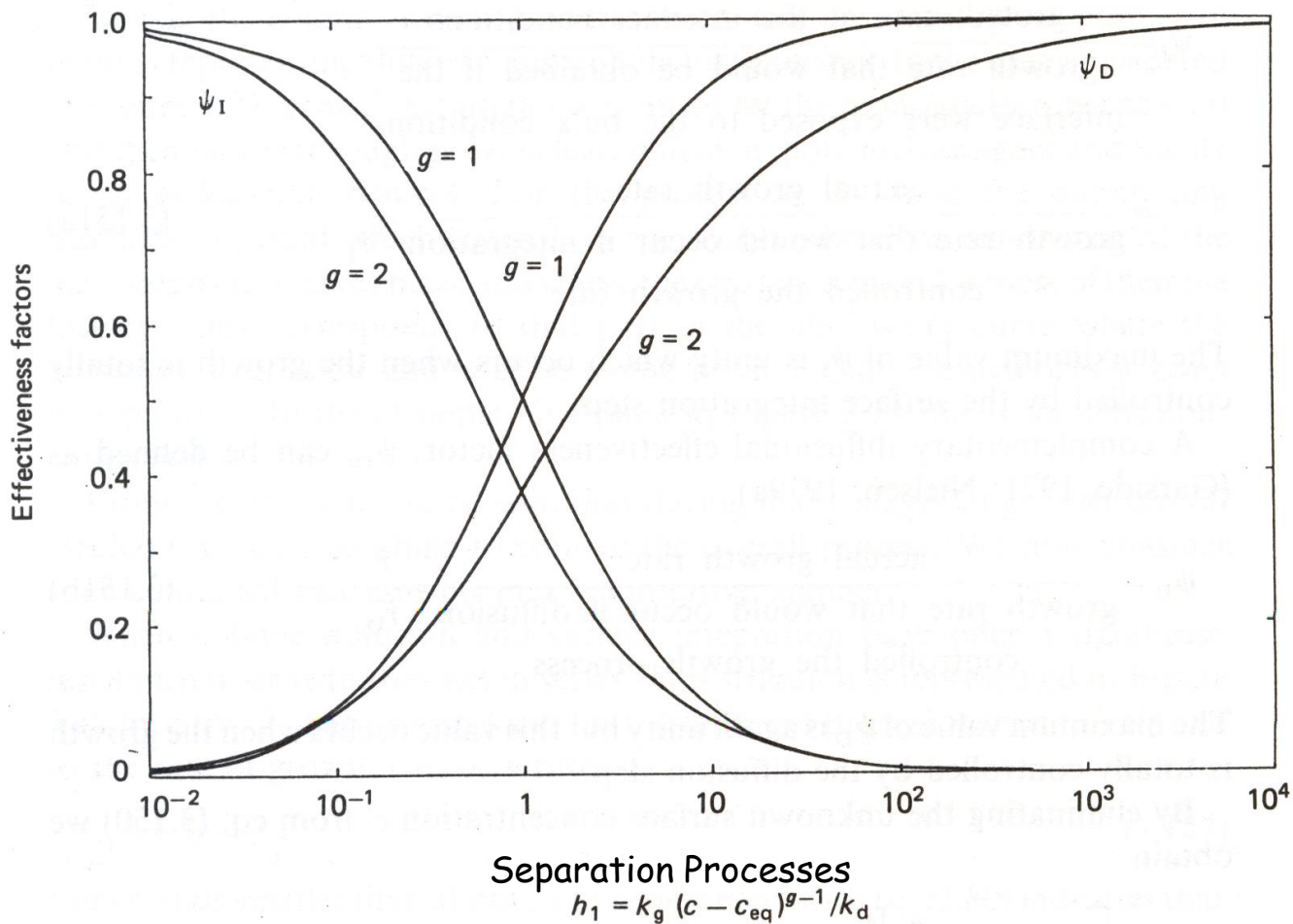
$$= \frac{\dot{r}}{\dot{r}_D}$$

For crystals $> 5\mu\text{m}$ $k_D = DV_m/\delta$

$\Psi_D < 0.1\mu\text{m}$ or $\Psi_I > 0.9$ rate determining step is surface integration

$\Psi_D > 0.1\mu\text{m}$ or $\Psi_I < 0.9$ both steps participate in the growth

$\Psi_D > 0.9\mu\text{m}$ or $\Psi_I < 0.1$ diffusion dominates growth process



At steady state, the concentration distribution on the surface of the crystal does not change. For this to happen, the rates due to diffusion and to surface integration, should be equal :

$$\dot{r} = k_d (c - c') = k_g (c' - c_{eq})^g$$

Introducing $S=c/c_{eq}$ and eliminating $S'=c'/c_{eq}$ it may be shown that the relationship between

$$\frac{(S - 1)}{\sqrt{\dot{r}}} \quad \sqrt{\dot{r}}$$

Is linear with slope $(k_d c_{eq})^{-1}$ and abscissa $(k_g c_{eq}^2)^{-1/2}$

Crystal Dissolution

- Rate of dissolution:

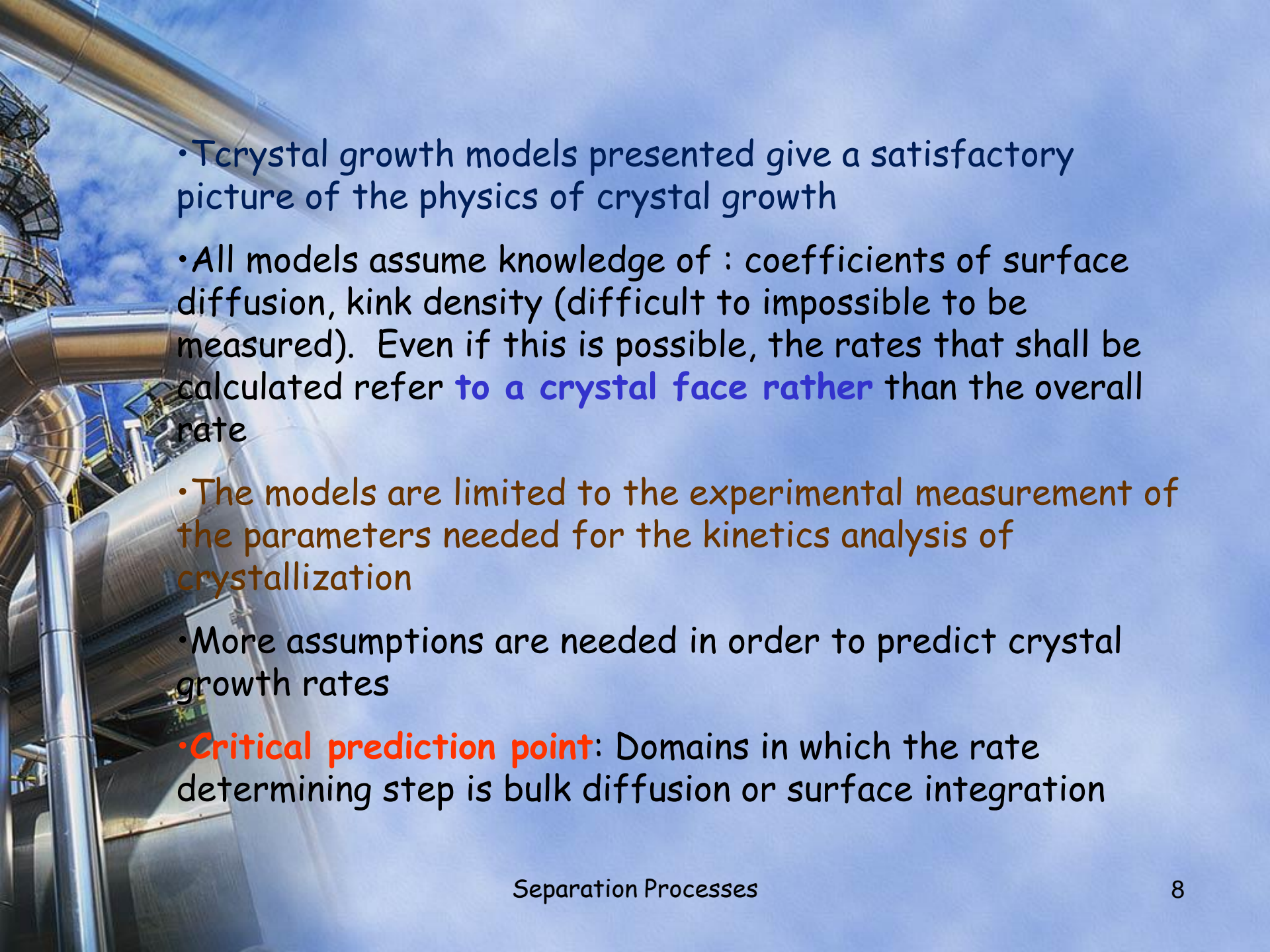
$$R_D = K_D(c^* - c)^d$$

d usually (but not necessarily) = 1

From the relationship giving the rate due to bulk diffusion

$$c_i = c - R_G/k_d$$

Replacement of the rate controlled by reaction

- 
- A photograph of an industrial distillation column and associated piping, set against a blue sky with light clouds. The column is a large, vertical, cylindrical vessel with a complex network of pipes and ladders around it. The scene is brightly lit, suggesting a clear day.
- Crystal growth models presented give a satisfactory picture of the physics of crystal growth
 - All models assume knowledge of : coefficients of surface diffusion, kink density (difficult to impossible to be measured). Even if this is possible, the rates that shall be calculated refer **to a crystal face rather** than the overall rate
 - The models are limited to the experimental measurement of the parameters needed for the kinetics analysis of crystallization
 - More assumptions are needed in order to predict crystal growth rates
 - **Critical prediction point**: Domains in which the rate determining step is bulk diffusion or surface integration

Combination of mechanisms

It is doubtful if only one mechanism is operational during crystal growth. Diffusional mass flux, N , to a crystallite of size r , according to Turnbull (1931) is:

$$N = K \left(\frac{dr}{dt} \right) = \frac{D\kappa c}{D + \kappa}$$

D : diffusion coefficient, K constant, κ mass transport coefficient at the interface, $N = \kappa(c_r - c^*)$

c_r , c^* , c : concentrations at the surface, equilibrium and in solution

Integration

$$\frac{r^2}{2D} + \frac{r}{\kappa} = Ktc$$

$$r \rightarrow 0$$

$$r \approx \kappa Ktc$$

i.e. crystal growth rate of very small crystallites is controlled by the interface.
For large values of r :

$$r \rightarrow \sqrt{2DKtc}$$

The importance of the surface

- Surface roughness

$$a = \frac{\xi \Delta H}{RT}$$

ξ : entropy factor, the binding energy of crystal layers

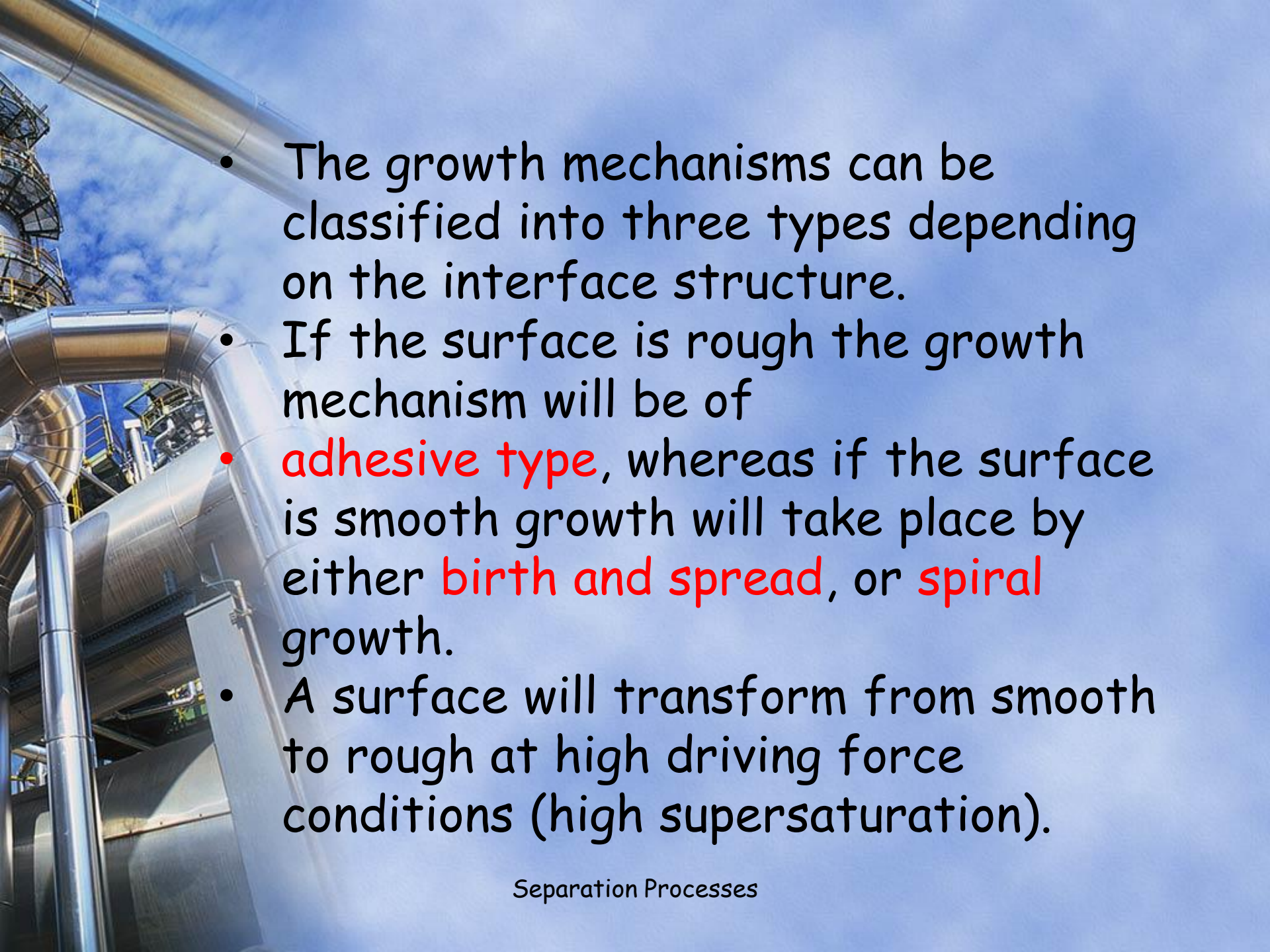
ΔH enthalpy of melting

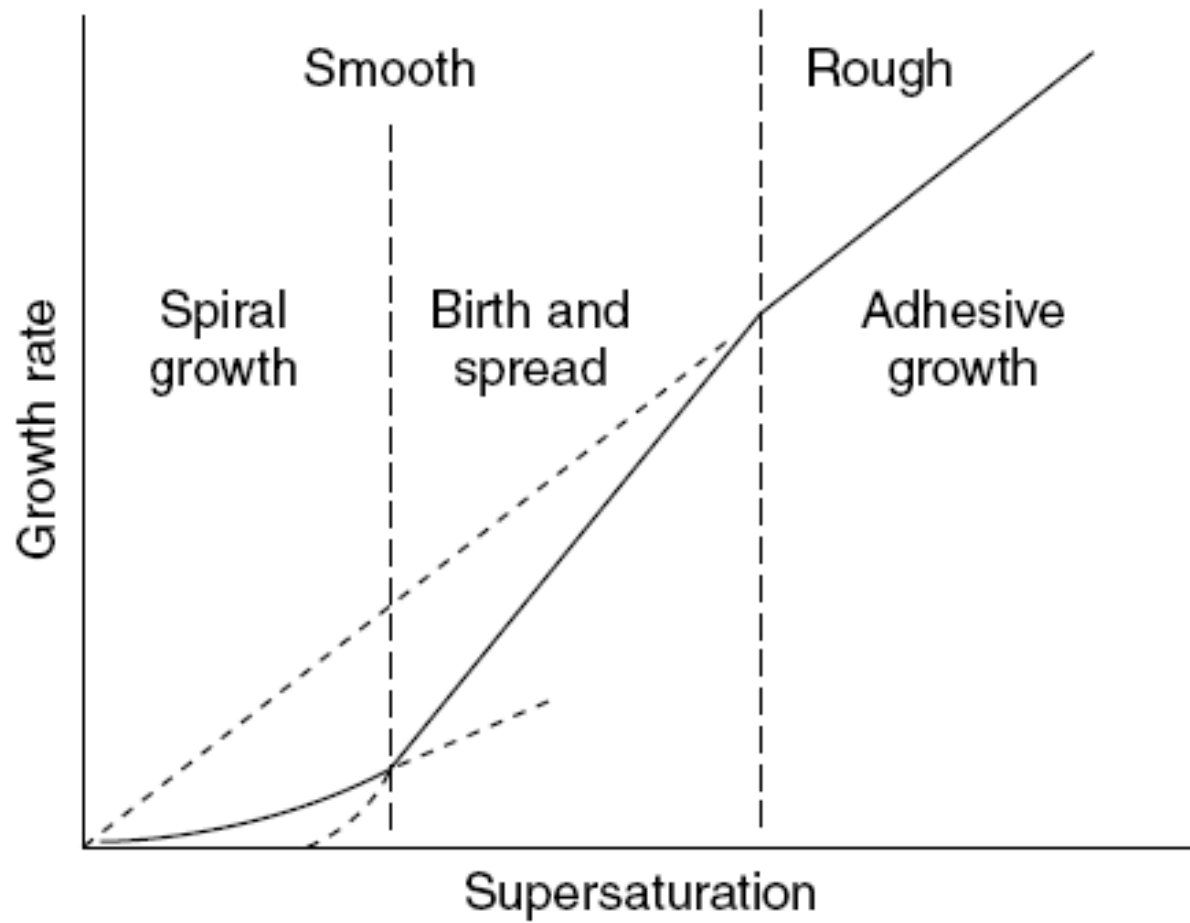
$\alpha < 2$ rough surfaces $u \propto \sigma$

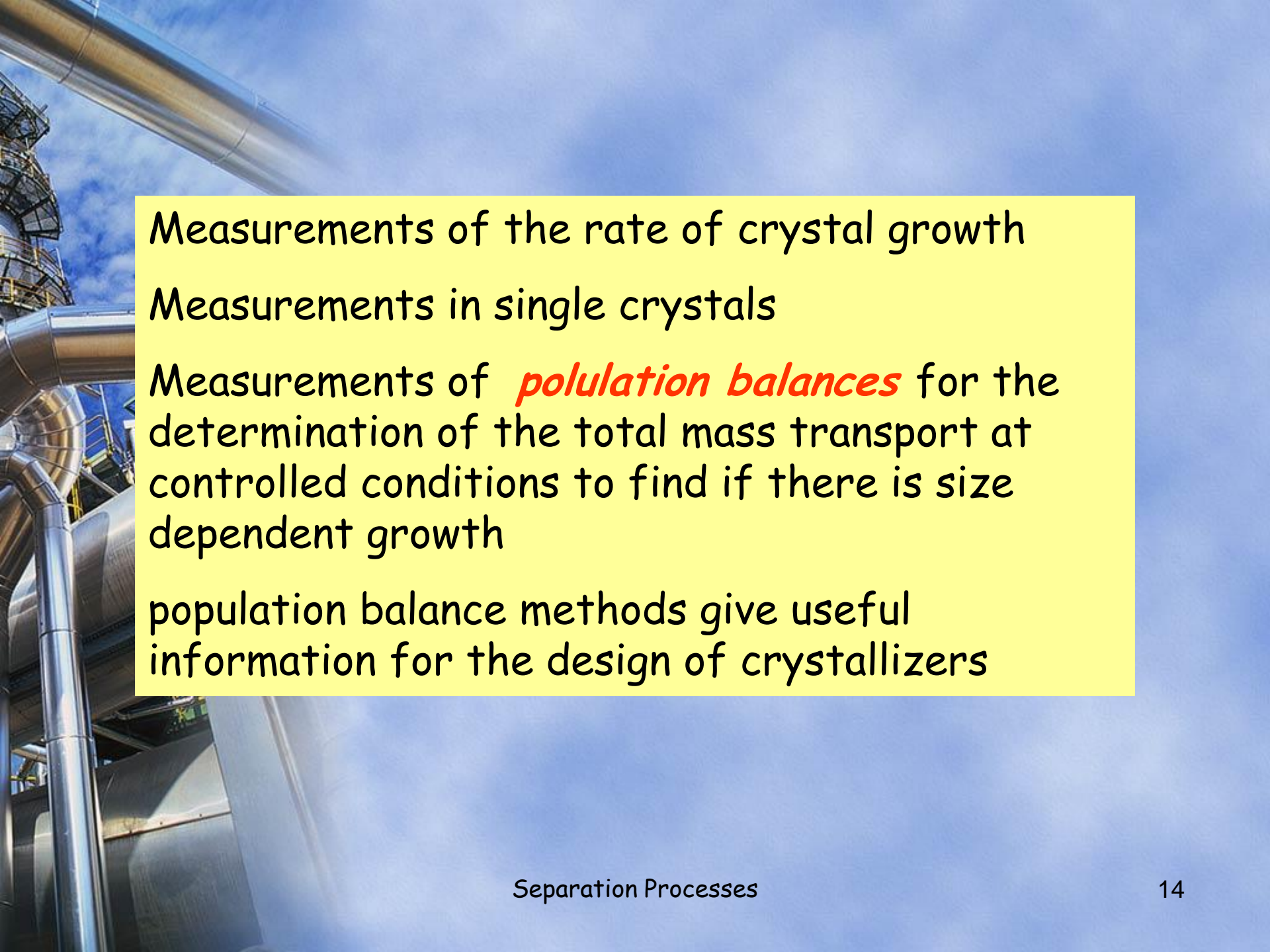
$\alpha > 5$ smooth surfaces, BCF, $u \propto \sigma^2 \tanh(B'/\sigma)$ and for low supersaturations $u \propto \sigma^2$

For $2 < \alpha < 5$ the birth and spread volume is valid

In practice: $u \propto \sigma^r$

- 
- The background of the slide is a photograph of an industrial facility, likely a refinery or chemical plant. It features several large, silver-colored metal pipes that curve and connect various pieces of equipment. In the upper left, there's a tall, cylindrical structure with a metal walkway or ladder around it. The sky is a clear, bright blue with some light, wispy clouds. The overall scene is brightly lit, suggesting a sunny day.
- The growth mechanisms can be classified into three types depending on the interface structure.
 - If the surface is rough the growth mechanism will be of
 - **adhesive type**, whereas if the surface is smooth growth will take place by either **birth and spread**, or **spiral growth**.
 - A surface will transform from smooth to rough at high driving force conditions (high supersaturation).



The background of the slide is a photograph of an industrial facility, likely a refinery or chemical plant. It features large, silver-colored metal pipes and structures, some with scaffolding, set against a clear blue sky with a few wispy clouds. The perspective is looking upwards and to the left.

Measurements of the rate of crystal growth

Measurements in single crystals

Measurements of *population balances* for the determination of the total mass transport at controlled conditions to find if there is size dependent growth

population balance methods give useful information for the design of crystallizers

Table 6.1. Some mean overall crystal growth rates expressed as a linear velocity

The supersaturation is expressed by $S = c/c^*$ with c and c^* as kg of crystallizing substance per kg of free water. The significance of the mean linear growth velocity, $\bar{v} (= \frac{1}{2}G)$, is explained by equation 6.61 and the values recorded here refer to crystals in the approximate size range 0.5–1 mm growing in the presence of other crystals. An asterisk (*) denotes that the growth rate is probably size dependent.

Crystallizing substance	°C	S	\bar{v} (m s ⁻¹)
(NH ₄) ₂ SO ₄ · Al ₂ (SO ₄) ₃ · 24H ₂ O	15	1.03	1.1 × 10 ^{-8*}
	30	1.03	1.3 × 10 ^{-8*}
	30	1.09	1.0 × 10 ^{-7*}
	40	1.08	1.2 × 10 ^{-7*}
NH ₄ NO ₃	40	1.05	8.5 × 10 ⁻⁷
(NH ₄) ₂ SO ₄	30	1.05	2.5 × 10 ^{-7*}
	60	1.05	4.0 × 10 ⁻⁷
	90	1.01	3.0 × 10 ⁻⁸
NH ₄ H ₂ PO ₄	20	1.06	6.5 × 10 ⁻⁸
	30	1.02	3.0 × 10 ⁻⁸
	30	1.05	1.1 × 10 ⁻⁷
	40	1.02	7.0 × 10 ⁻⁸
MgSO ₄ · 7H ₂ O	20	1.02	4.5 × 10 ^{-8*}
	30	1.01	8.0 × 10 ^{-8*}
	30	1.02	1.5 × 10 ^{-7*}
NiSO ₄ · (NH ₄) ₂ SO ₄ · 6H ₂ O	25	1.03	5.2 × 10 ⁻⁹
	25	1.09	2.6 × 10 ⁻⁸
	25	1.20	4.0 × 10 ⁻⁸
K ₂ SO ₄ · Al ₂ (SO ₄) ₃ · 24H ₂ O	15	1.04	1.4 × 10 ^{-8*}
	30	1.04	2.8 × 10 ^{-8*}
	30	1.09	1.4 × 10 ^{-7*}
	40	1.03	5.6 × 10 ^{-8*}
KCl	20	1.02	2.0 × 10 ⁻⁷
	40	1.01	6.0 × 10 ⁻⁷
KNO ₃	20	1.05	4.5 × 10 ⁻⁸
	40	1.05	1.5 × 10 ⁻⁷
K ₂ SO ₄	20	1.09	2.8 × 10 ^{-8*}
	20	1.18	1.4 × 10 ^{-7*}
	30	1.07	4.2 × 10 ^{-8*}
	50	1.06	7.0 × 10 ^{-8*}
	50	1.12	3.2 × 10 ^{-7*}
KH ₂ PO ₄	30	1.07	3.0 × 10 ⁻⁸
	30	1.21	2.9 × 10 ⁻⁷
	40	1.06	5.0 × 10 ⁻⁸
	40	1.18	1.4 × 10 ⁻⁷

Table 6.1. (Continued)

<i>Crystallizing substance</i>	$^{\circ}\text{C}$	<i>S</i>	\bar{v} (m s^{-1})
NaCl	50	1.002	2.5×10^{-8}
	50	1.003	6.5×10^{-8}
	70	1.002	9.0×10^{-8}
	70	1.003	1.5×10^{-7}
$\text{Na}_2\text{S}_2\text{O}_3 \cdot 5\text{H}_2\text{O}$	30	1.02	1.1×10^{-7}
	30	1.08	5.0×10^{-7}
Citric acid monohydrate	25	1.05	3.0×10^{-8}
	30	1.01	1.0×10^{-8}
	30	1.05	4.0×10^{-8}
Sucrose	30	1.13	$1.1 \times 10^{-8*}$
	30	1.27	$2.1 \times 10^{-8*}$
	70	1.09	9.5×10^{-8}
	70	1.15	1.5×10^{-7}

Mass growth rates, R_G [$\text{kg m}^{-2}\text{s}^{-1}$]
Mean linear growth rate u [ms^{-1}]
Overall linear growth rate G [ms^{-1}]

$$R_G = K_G \Delta c^g = \frac{1}{A} \cdot \frac{dm}{dt} = \frac{3\alpha}{\beta} \cdot \rho_c G = \frac{3\alpha}{\beta} \rho_c \frac{dL}{dt} = \frac{6\alpha}{\beta} \cdot \rho_c \frac{dr}{dt} = \frac{6\alpha}{\beta} \cdot \rho_c \bar{v}$$

$$m = \alpha \rho_c L^3$$

$$dm = 3\alpha \rho_c L^2 dL$$

$$A = \beta L^2$$

$$dA = 2\beta L dL$$

For spheres and cubes $6\alpha/\beta=1$,
for octahedral =0.816

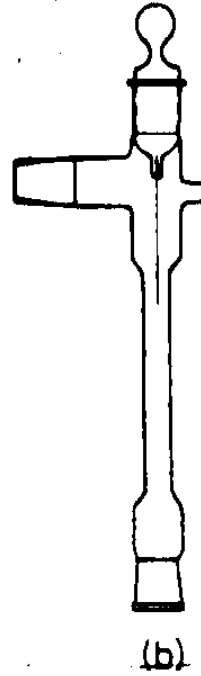
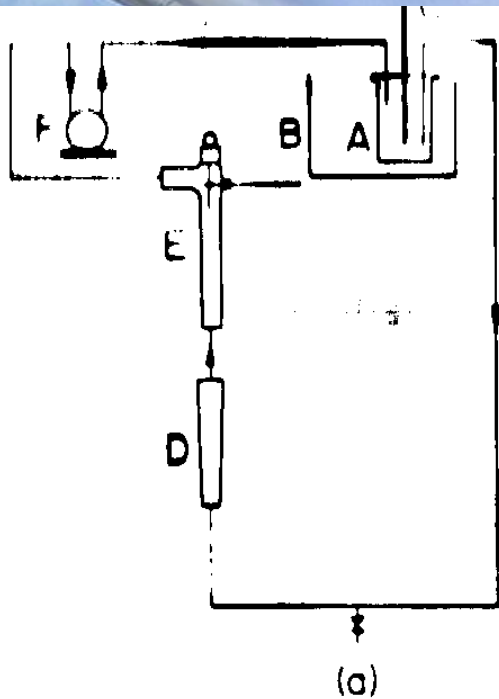
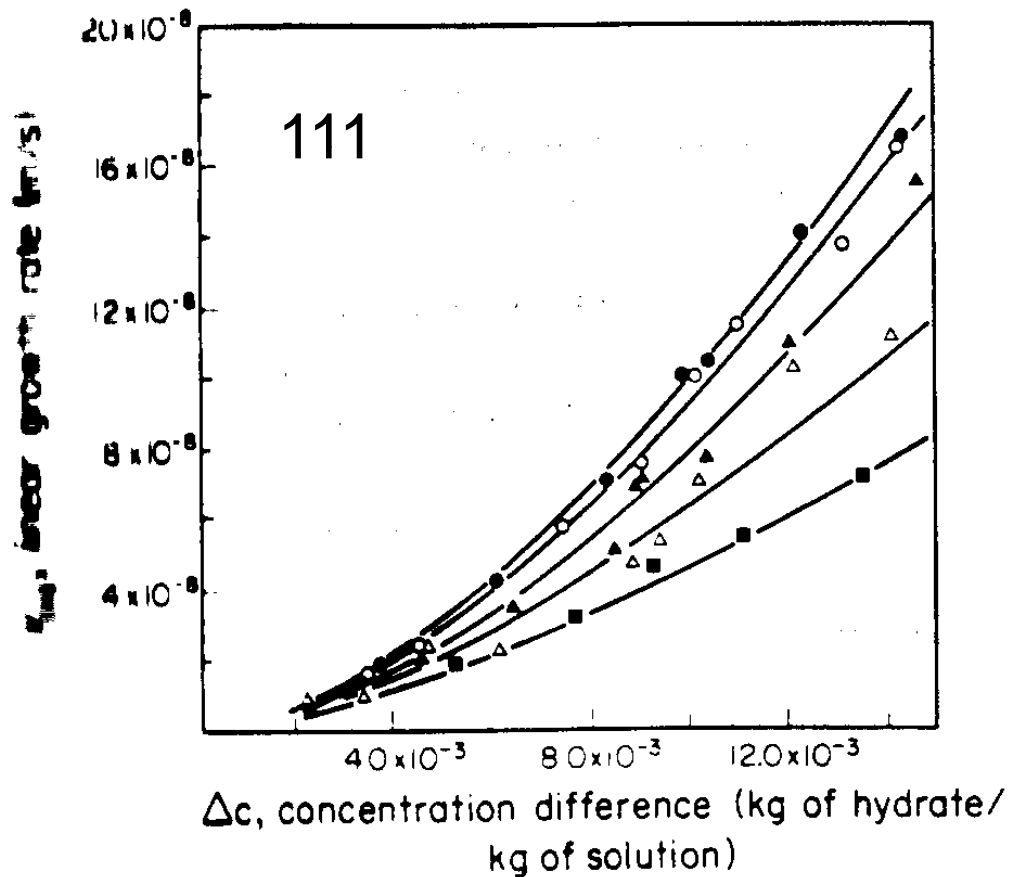


Figure 6.12. Single-crystal growth cell: (a) complete circuit, (b) the cell. A, solution reservoir; (B), thermostat bath; C, thermometer; D, flow meter; E, cell; F, pump. (After Mullin and Amatavivadhana, 1967; Mullin and Garside, 1967)



Έδρες με υψηλούς δείκτες κρυσταλλώνονται ταχύτερα

$$v_{111} = K\Delta c^g$$

Figure 6.13. Face growth rates of single crystals of potash alum at 32°C. Solution velocities: ● = 0.127, ○ = 0.120, ▲ = 0.064, △ = 0.022, ■ = 0.006 m s⁻¹. (After Mullin and Garside, 1967)

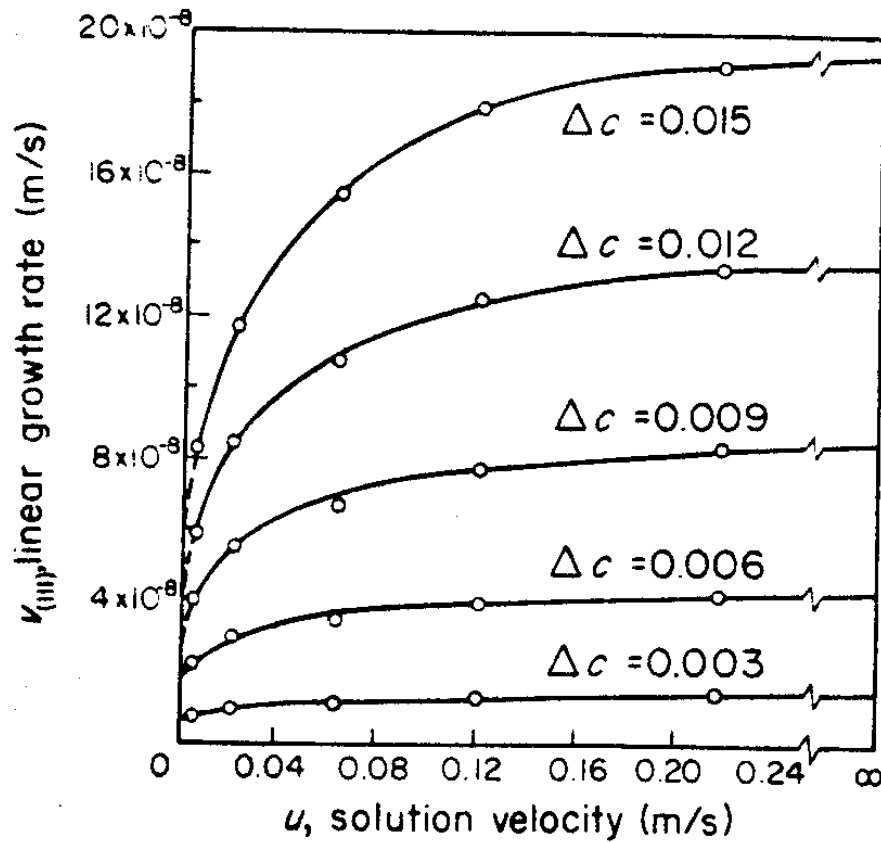


Figure 6.14. Effect of solution velocity on the (111) face growth rate of potash alum crystals at 32°C. (After Mullin and Garside, 1967)

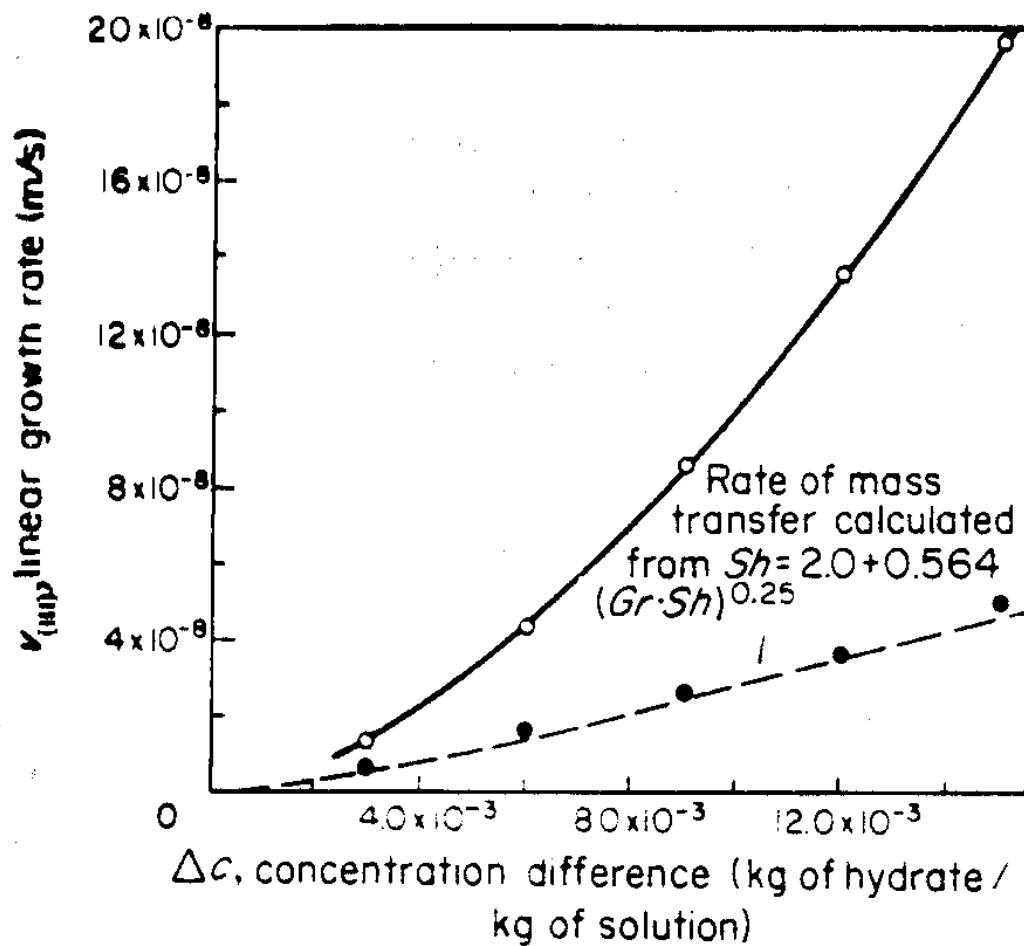


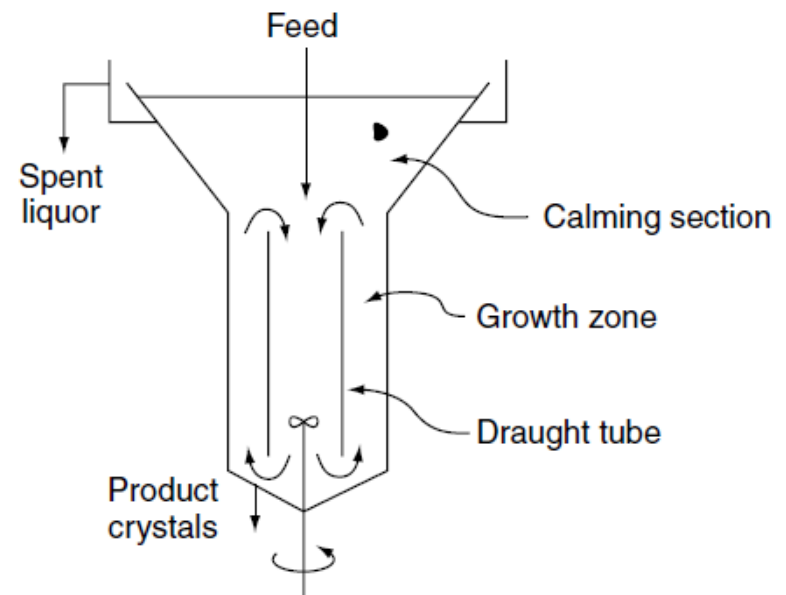
Figure 6.15. Extrapolated growth rates of potash alum crystals at limiting velocities (○ = $u \rightarrow \infty$, ● = $u \rightarrow 0$) (After Mullin and Garside, 1967)

The typical **agitated cooling crystalliser**, has an upper conical section which reduces the upward velocity of liquor and prevents the crystalline product from being swept out with the spent liquor.

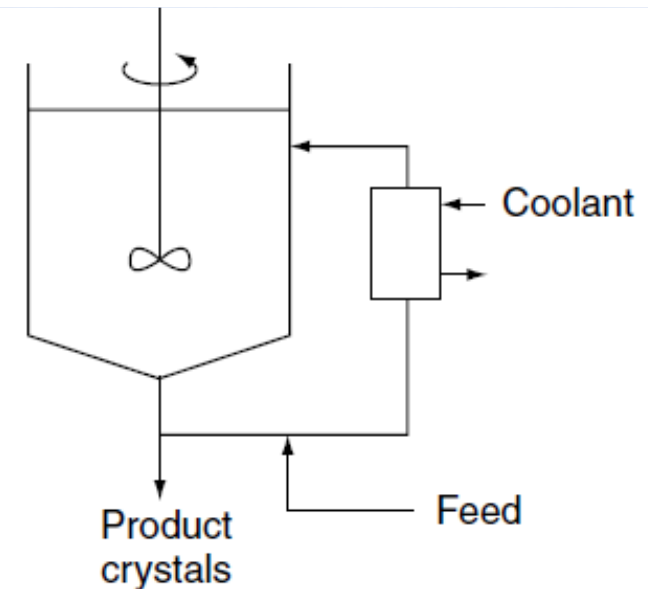
An agitator, located in the lower region of a draught tube circulates the crystal slurry through the growth zone of the crystalliser; Cooling surfaces may be provided if required. External circulation, as shown in Figure , allows good mixing inside the unit and promotes high rates of heat transfer between liquor and coolant, and an internal agitator may be installed in the crystallisation tank if required.

Because the liquor velocity in the tubes is high, low temperature differences are usually adequate, and encrustation on heat transfer surfaces is reduced considerably.

Batch or continuous operation may be employed.



(a) Internal circulation through a draught tube

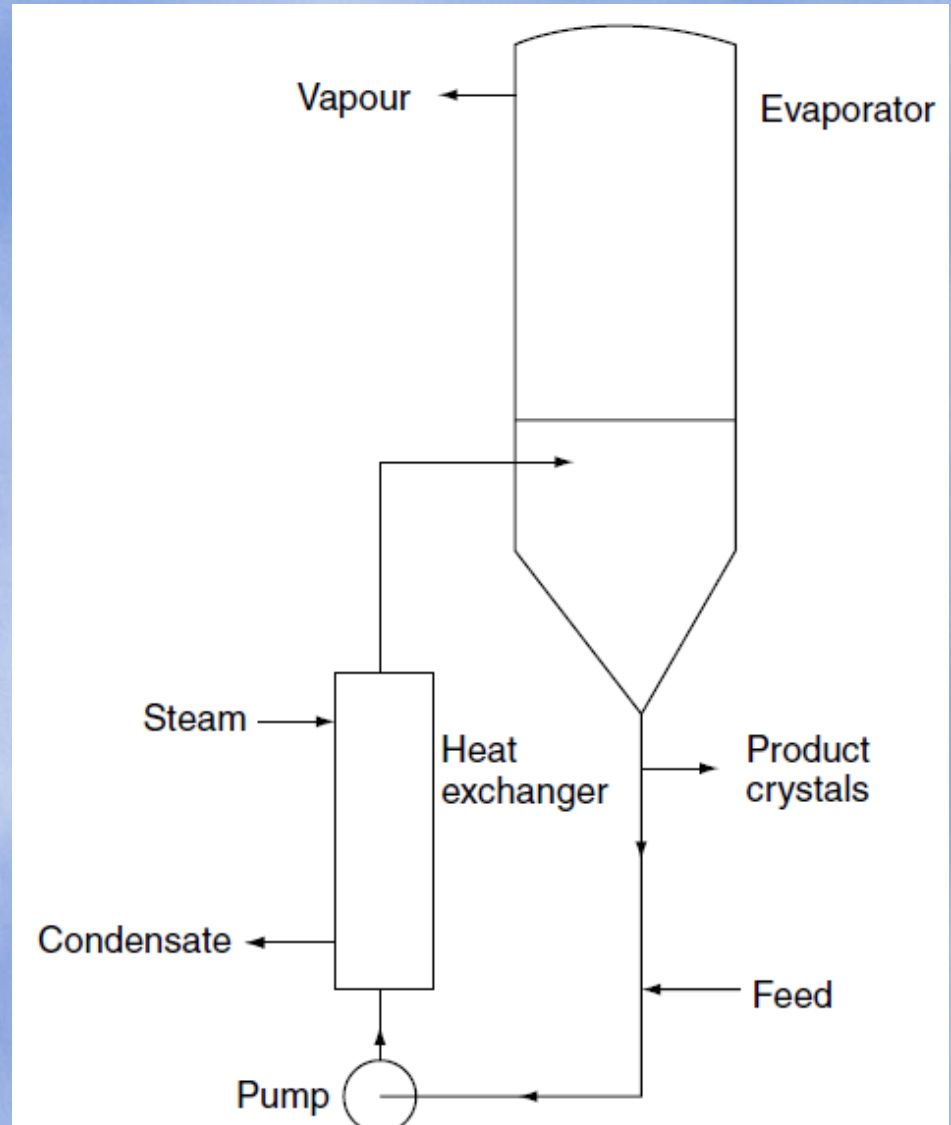


(b) External circulation through a heat exchanger

Forced-circulation crystallisers

A **Swenson forced-circulation crystalliser** operating at reduced pressure is shown in the Figure.

A high recirculation rate through the external heat exchanger is used to provide good heat transfer with minimal encrustation. The crystal magma is circulated from the lower conical section of the evaporator body, through the vertical tubular heat exchanger, and reintroduced tangentially into the evaporator below the liquor level to create a swirling action and prevent flashing. Feed-stock enters on the pump inlet side of the circulation system and product crystal magma is removed below the conical section.

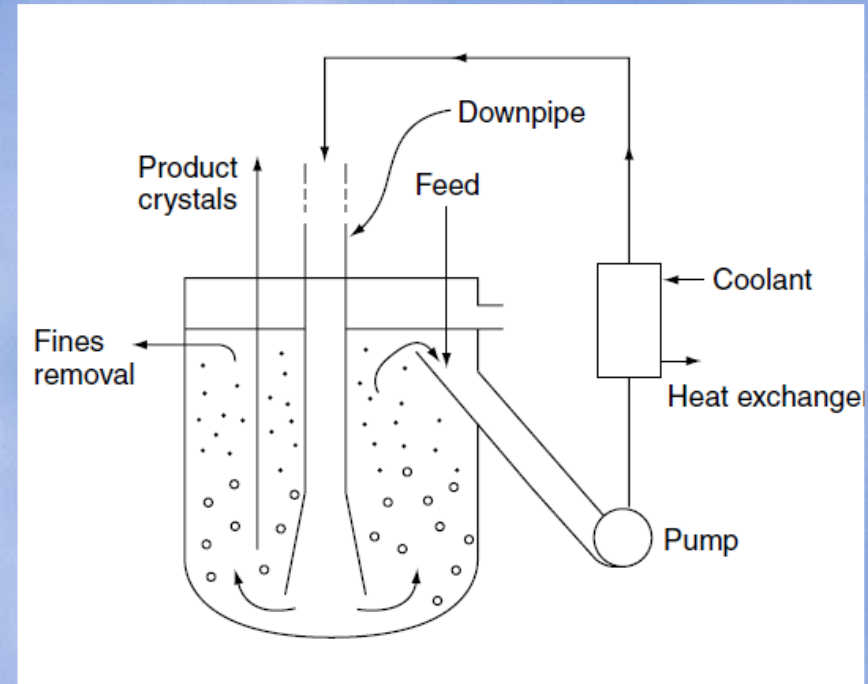


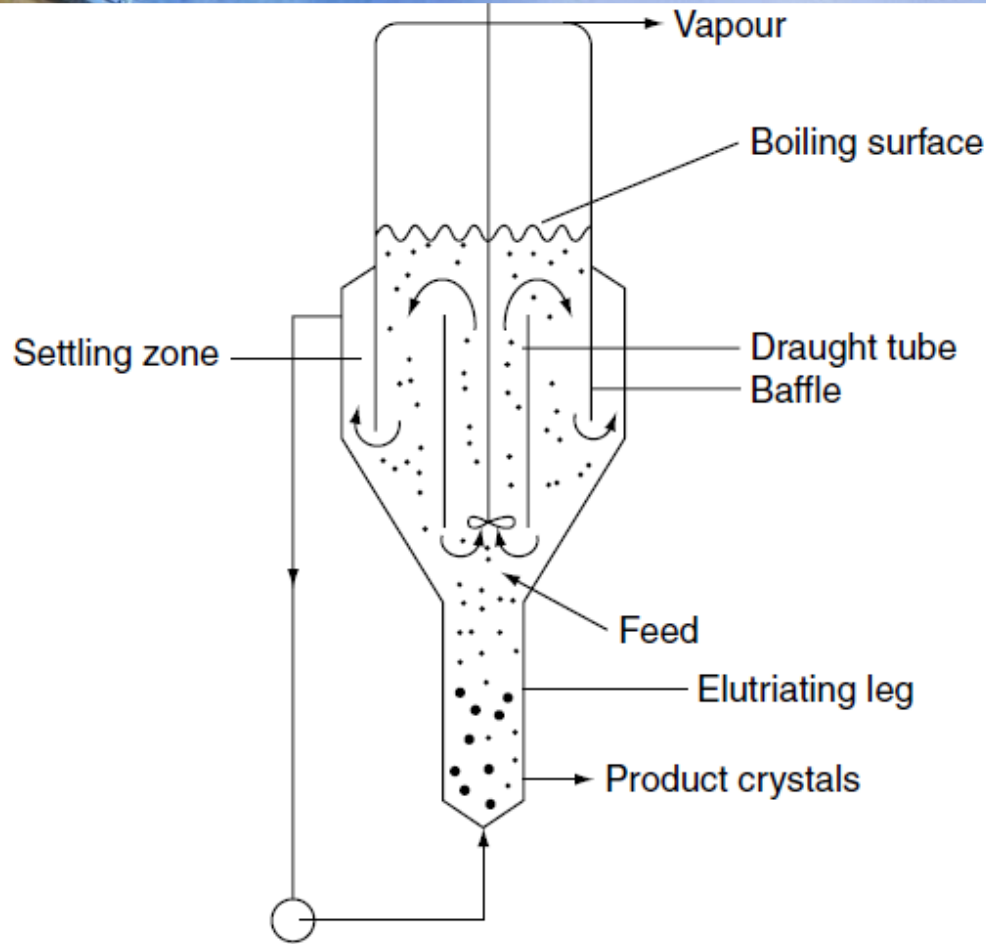
Fluidised-bed crystallisers

In an **Oslo fluidised-bed crystalliser**, a bed of crystals is suspended in the vessel by the upward flow of supersaturated liquor in the annular region surrounding a central downcomer, as shown in the Figure. Although originally designed as classifying crystallisers, **fluidised-bed Oslo units** are frequently operated in a mixed-suspension mode to improve productivity, although this reduces product crystal size.

With the classifying mode of operation, hot, concentrated feed solution is fed into the vessel at a point directly above the inlet to the circulation pipe. Saturated solution from the upper regions of the crystalliser, together with the small amount of feedstock, is circulated through the tubes of the heat exchanger and cooled by forced circulation of water or brine. In this way, the solution becomes supersaturated although care must be taken to avoid spontaneous nucleation.

Product crystal magma is removed from the lower regions of the vessel



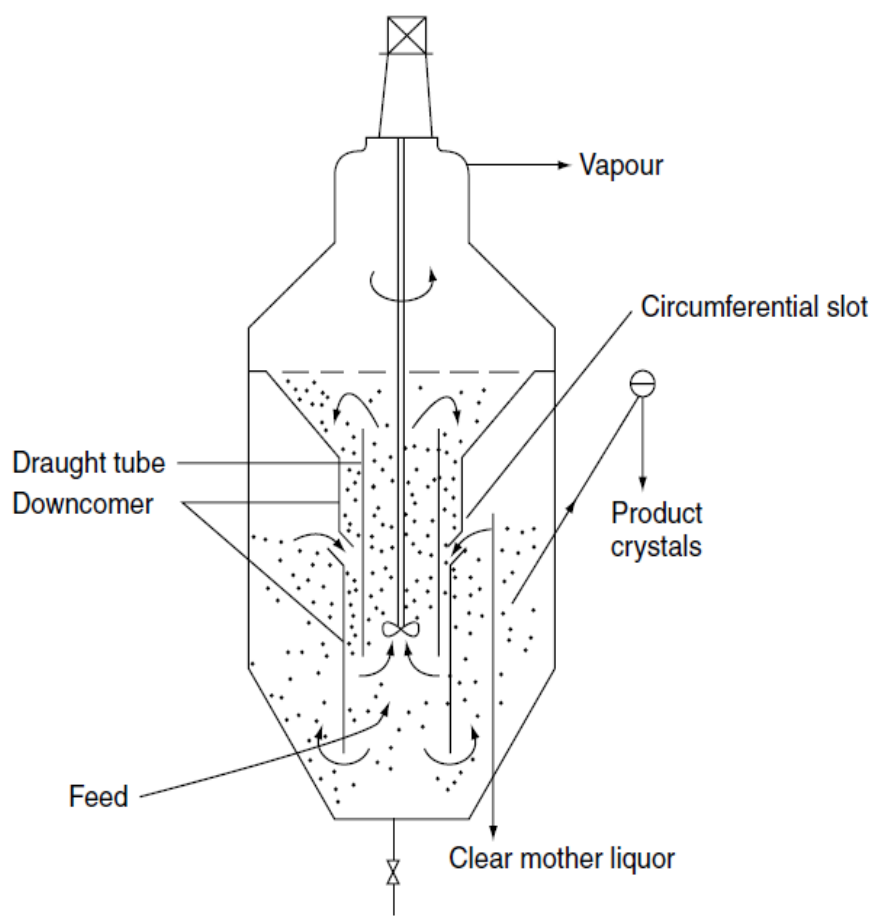


A relatively slow-speed propeller agitator is located in a draught tube that extends to a small distance below the liquor level. Hot, concentrated feed-stock, enters at the base of the draught tube, and the steady movement of magma and feed-stock to the surface of the liquor produces a gentle, uniform boiling action over the whole cross-sectional area of the crystallizer.

The degree of supercooling thus produced is less than 1 deg K and, in the absence of violent vapor flashing, both excessive nucleation and salt build-up on the inner walls are minimized.

The internal baffle forms an annular space free of agitation and provides a settling zone for regulating the magma density and controlling the removal of excess nuclei. An integral elutriating leg may be installed below the crystallization zone to effect some degree of product classification

Swenson draught-tube-baffled (DTB) crystalliser



is a draught-tube vacuum unit in which two liquor flow circuits are created by concentric pipes: an outer ejector tube with a circumferential slot, and an inner guide tube in which circulation is effected by a variable-speed agitator.

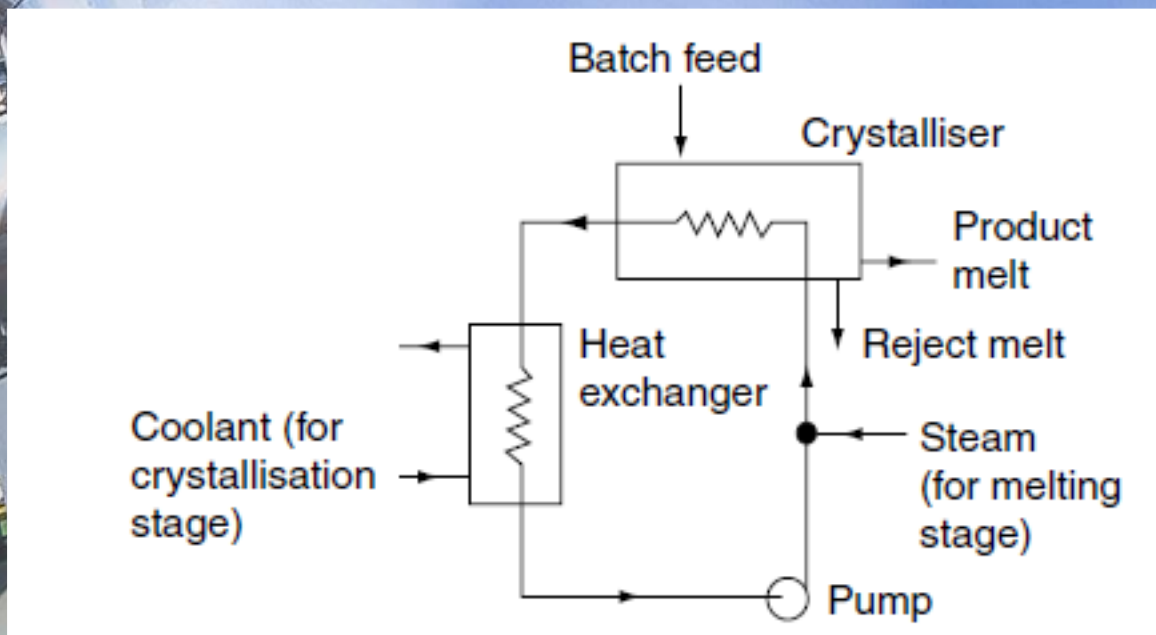
The principle of the Oslo crystalliser is utilised in the growth zone, partial classification occurs in the lower regions, and fine crystals segregate in the upper regions. The primary circuit is created by a fast upward flow of liquor in the guide tube and a downward flow in the annulus. In this way, liquor is drawn through the slot between the ejector tube and the baffle, and a secondary flow circuit is formed in the lower region of the vessel. Feedstock is introduced into the draught tube and passes into the vaporiser

section where flash evaporation takes place. In this way, nucleation occurs in this region, and the nuclei are swept into the primary circuit. Mother liquor may be drawn off by way of a control valve that provides a means of controlling crystal slurry density

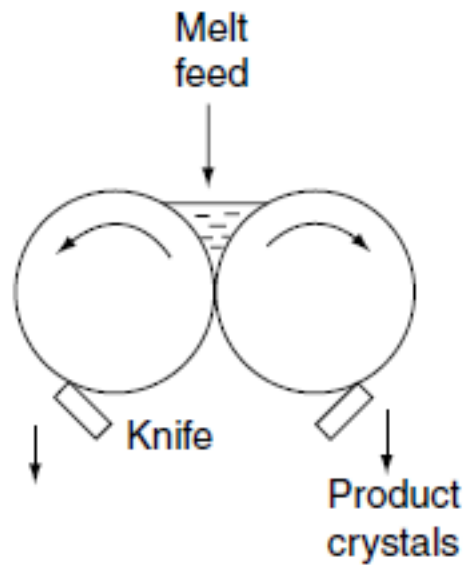
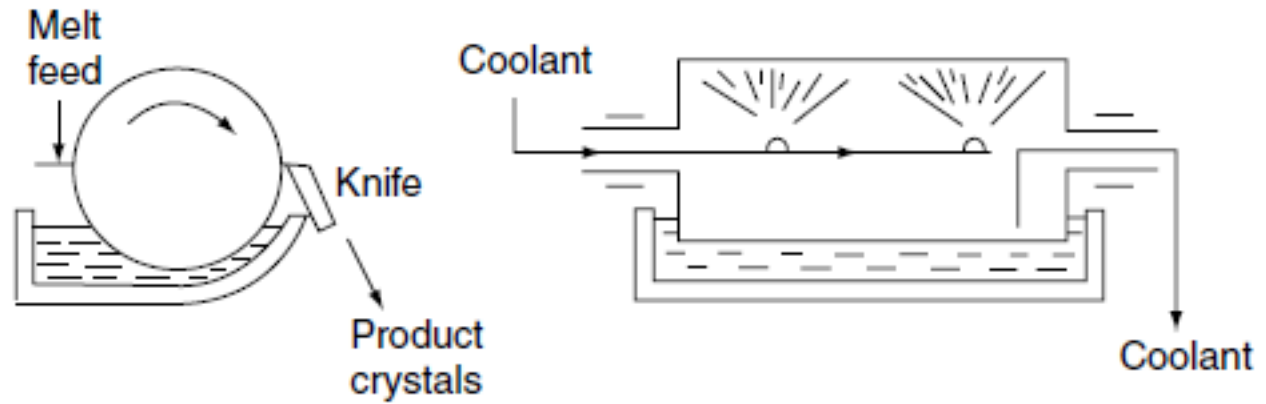
Standard-Messo turbulence crystalliser



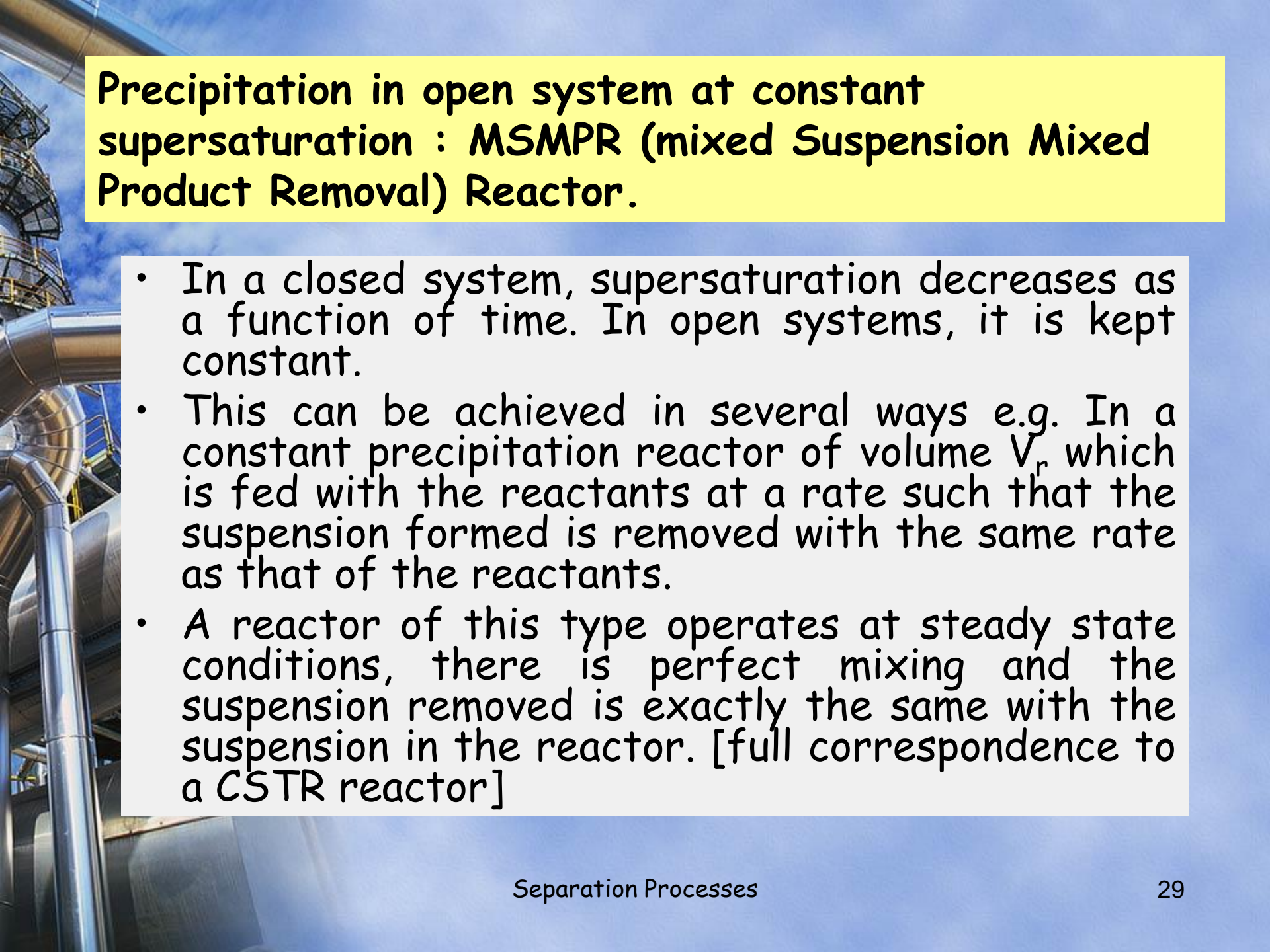
Two basic techniques of melt crystallisation are:
(a) gradual deposition of a crystalline layer on a chilled surface in a static or laminar flowing melt, and
(b) fast generation of discrete crystals in the body of an agitated vessel.



Batch cooling crystallisation of melts:
flow diagram for the Proabd refiner



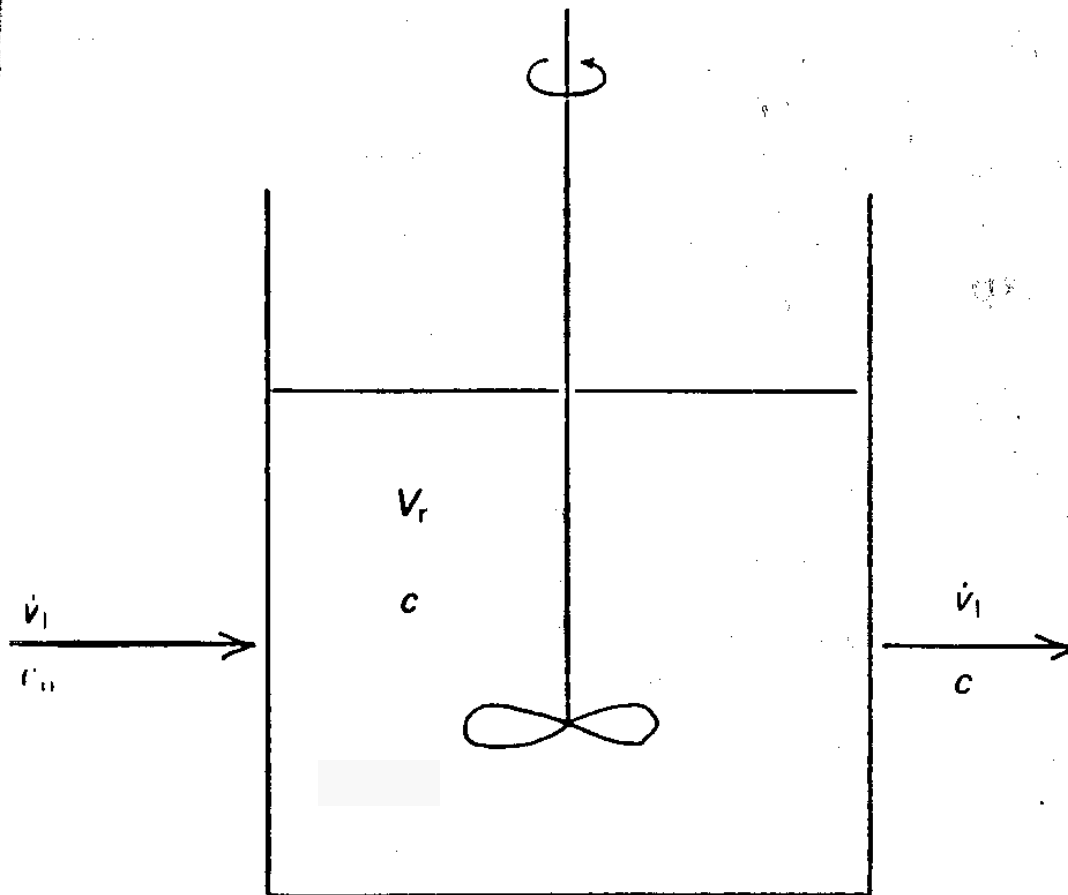
Feed and discharge arrangements for drum crystallisers



Precipitation in open system at constant supersaturation : MSMPR (mixed Suspension Mixed Product Removal) Reactor.

- In a closed system, supersaturation decreases as a function of time. In open systems, it is kept constant.
- This can be achieved in several ways e.g. In a constant precipitation reactor of volume V_r which is fed with the reactants at a rate such that the suspension formed is removed with the same rate as that of the reactants.
- A reactor of this type operates at steady state conditions, there is perfect mixing and the suspension removed is exactly the same with the suspension in the reactor. [full correspondence to a CSTR reactor]

Αντιδραστήρας
MSMPR (Mixed
Suspension Mixed
Product Removal)



Schematic representation of an MSMPR precipitation reactor of effective volume V_r being fed by a solution of concentration c_0 at rate \dot{v}_1 and suspension discharge at rate \dot{v}_1 with solute concentration c

Population balance

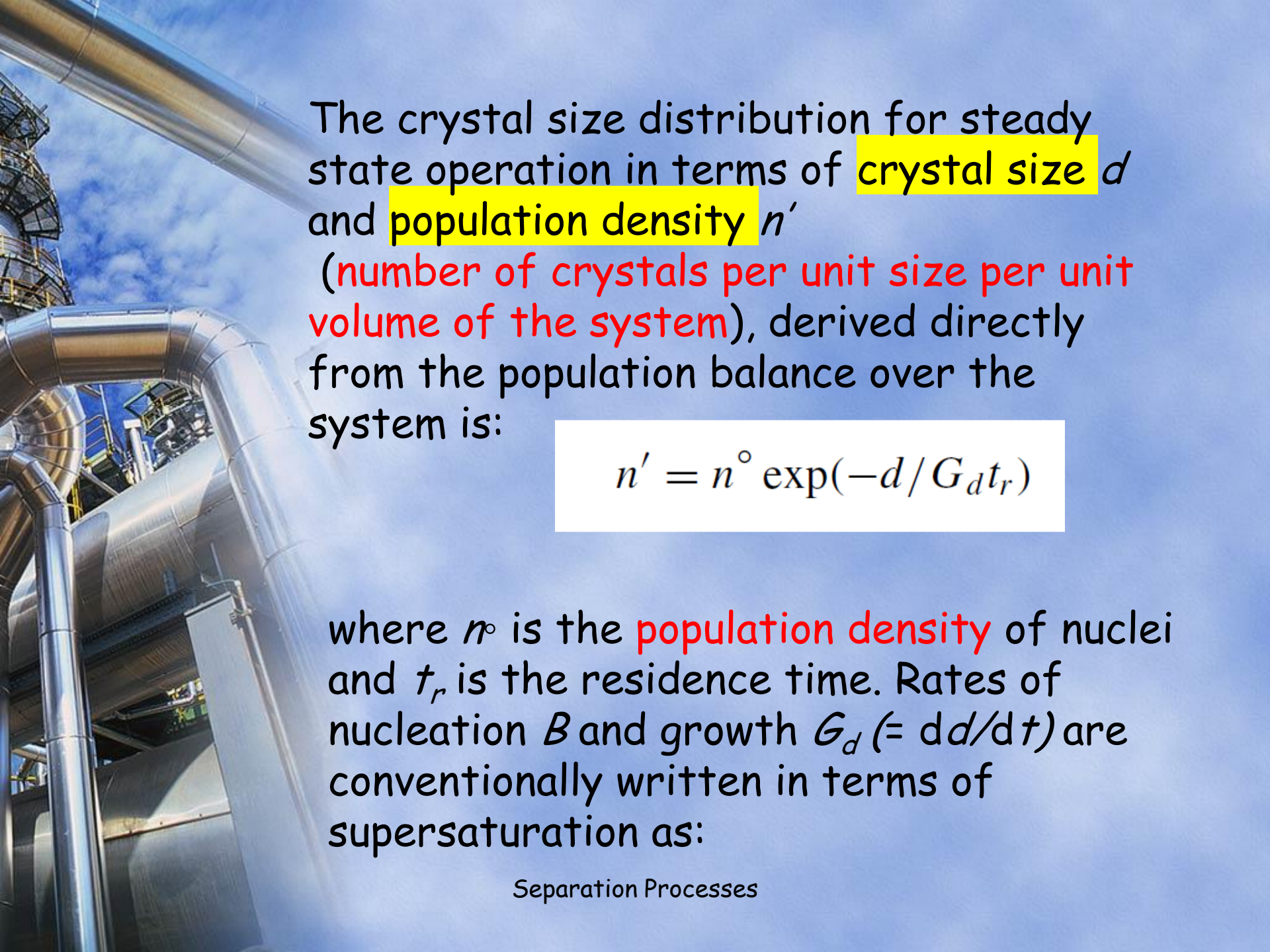
Growth and nucleation interact in a crystalliser in which both contribute to the final crystal size distribution (CSD) of the product.

The importance of the population balance is widely acknowledged.

This is most easily appreciated by reference to the simple,

idealised case of a mixed-suspension, mixed-product removal (MSMPR) crystalliser operated continuously in the steady state, where

- no crystals are present in the feed stream
- all crystals are of the same shape
- no crystals break down by attrition
- crystal growth rate is independent of crystal size.

The background of the slide is a photograph of an industrial facility, likely a refinery or chemical plant. It features several large, silver-colored metal pipes that curve and connect various pieces of equipment. The sky is a clear, bright blue with some light, wispy clouds. The overall scene is brightly lit, suggesting a sunny day.

The crystal size distribution for steady state operation in terms of crystal size d and population density n'

(number of crystals per unit size per unit volume of the system), derived directly from the population balance over the system is:

$$n' = n^{\circ} \exp(-d/G_d t_r)$$

where n° is the population density of nuclei and t_r is the residence time. Rates of nucleation B and growth $G_d (= dd/dt)$ are conventionally written in terms of supersaturation as:

$$B = k_1 \Delta c^b$$

$$G_d = k_2 \Delta c^s$$

These empirical expressions may be combined to give:

$$B = k_3 G^i$$

όπου $i = b/s$ and $k_3 = k_1/k_2^i$

b and s are the kinetic orders of nucleation and growth, respectively, and i is the relative kinetic order. The relationship between nucleation and growth may be expressed as:

$$B = n^{\circ} G_d$$

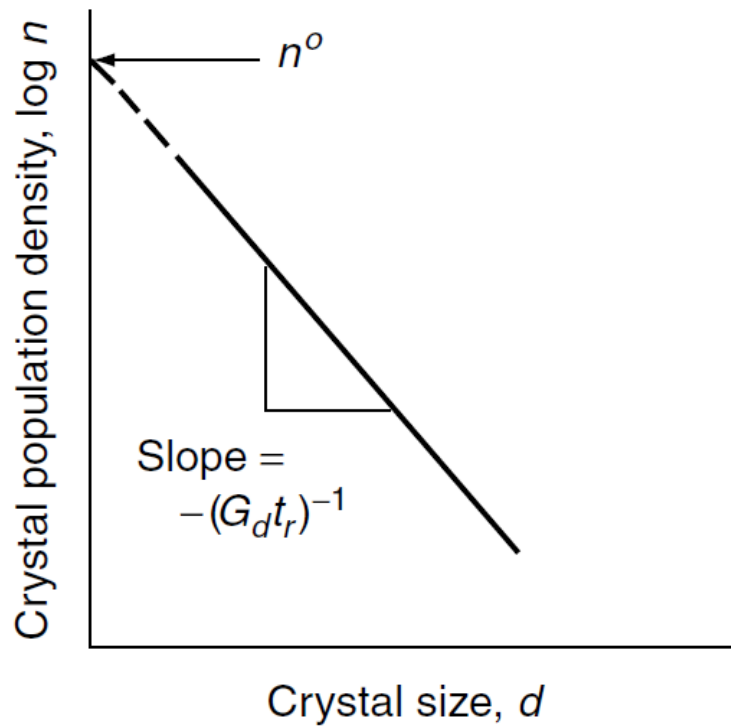
$$n^{\circ} = k_4 G_d^{i-1}$$

In this way, experimental measurement of crystal size distribution, recorded on a number basis, in a steady-state MSMPR crystalliser can be used to quantify nucleation and growth rates.

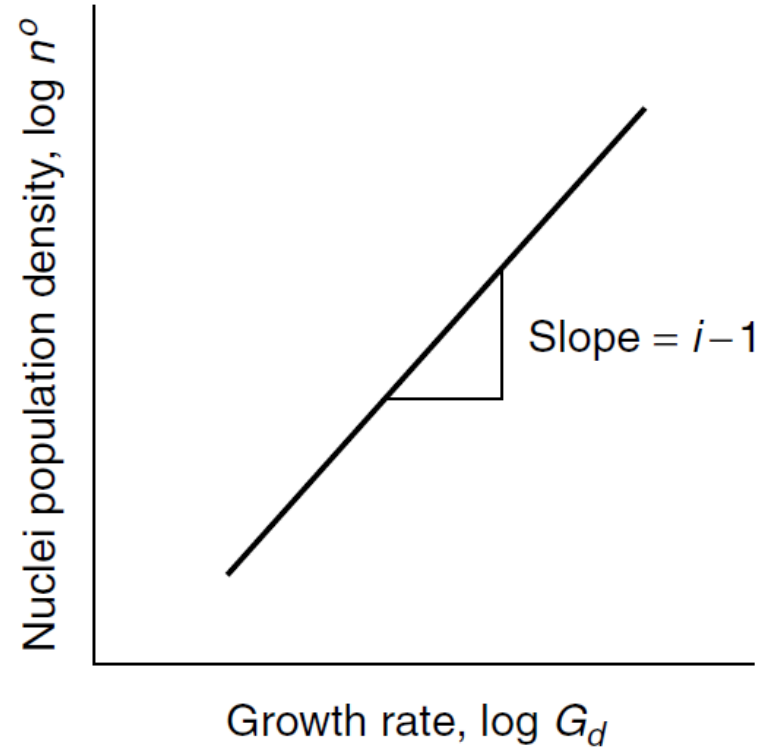
A plot of $\log n$ against d should give a straight line of slope $-(G_d t_r)^{-1}$ with an intercept at $d = 0$ equal to n° and, if the residence time t_r is known, the crystal growth rate G_d can be calculated.

Similarly, a plot of $\log n^{\circ}$ against $\log G_d$ should give a straight line of slope $(i - 1)$ and, if the order of the growth process s is known, the order of nucleation b may be calculated.

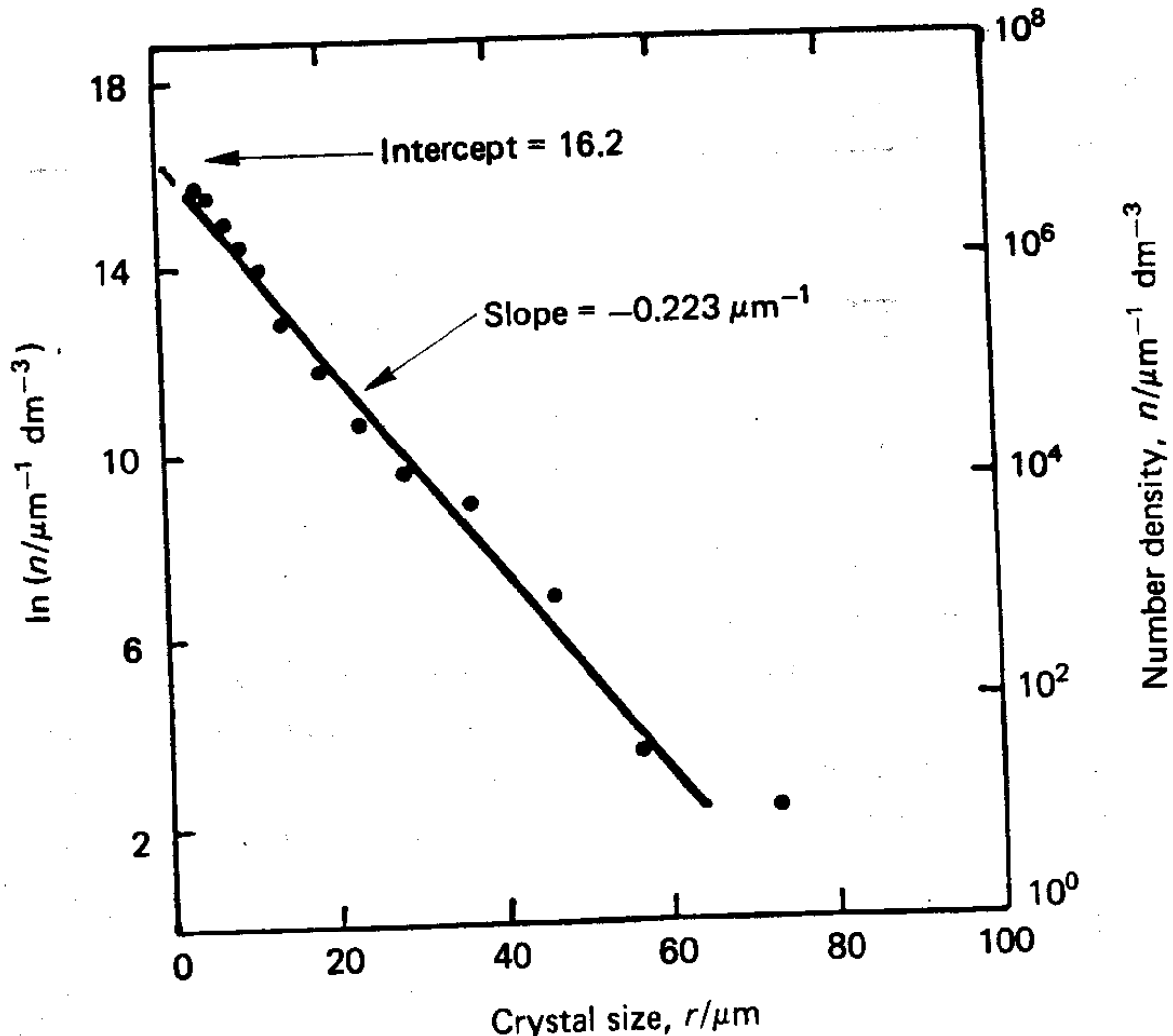
Population plots for a continuous mixed-suspension mixed-product removal (MSMPR) crystalliser



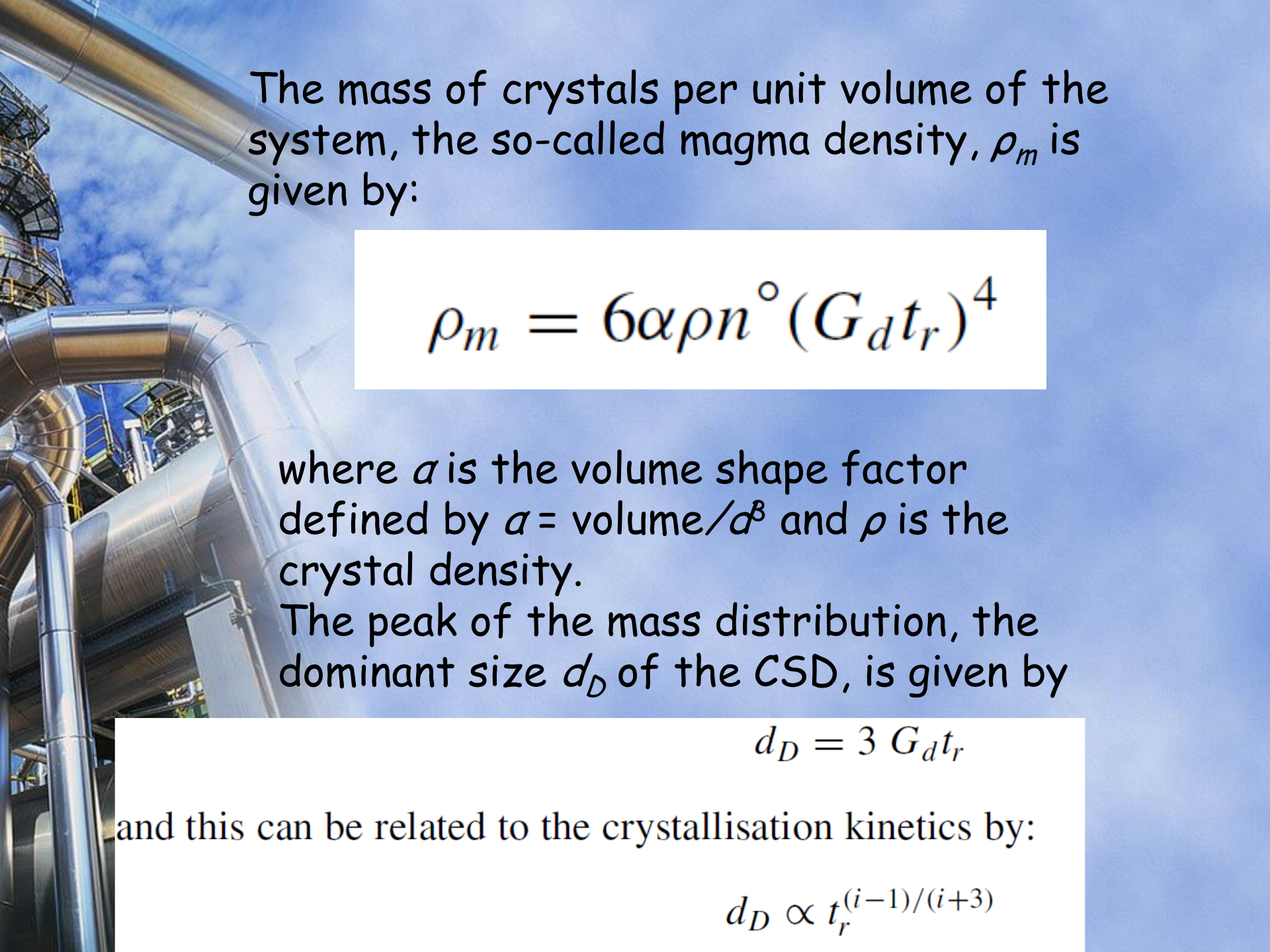
(a) Crystal size distribution



(b) Nucleation and growth kinetics



Steady-state crystal size distribution of calcium oxalate precipitated in a MSMPR crystallizer



The mass of crystals per unit volume of the system, the so-called magma density, ρ_m is given by:

$$\rho_m = 6\alpha\rho n^\circ (G_d t_r)^4$$

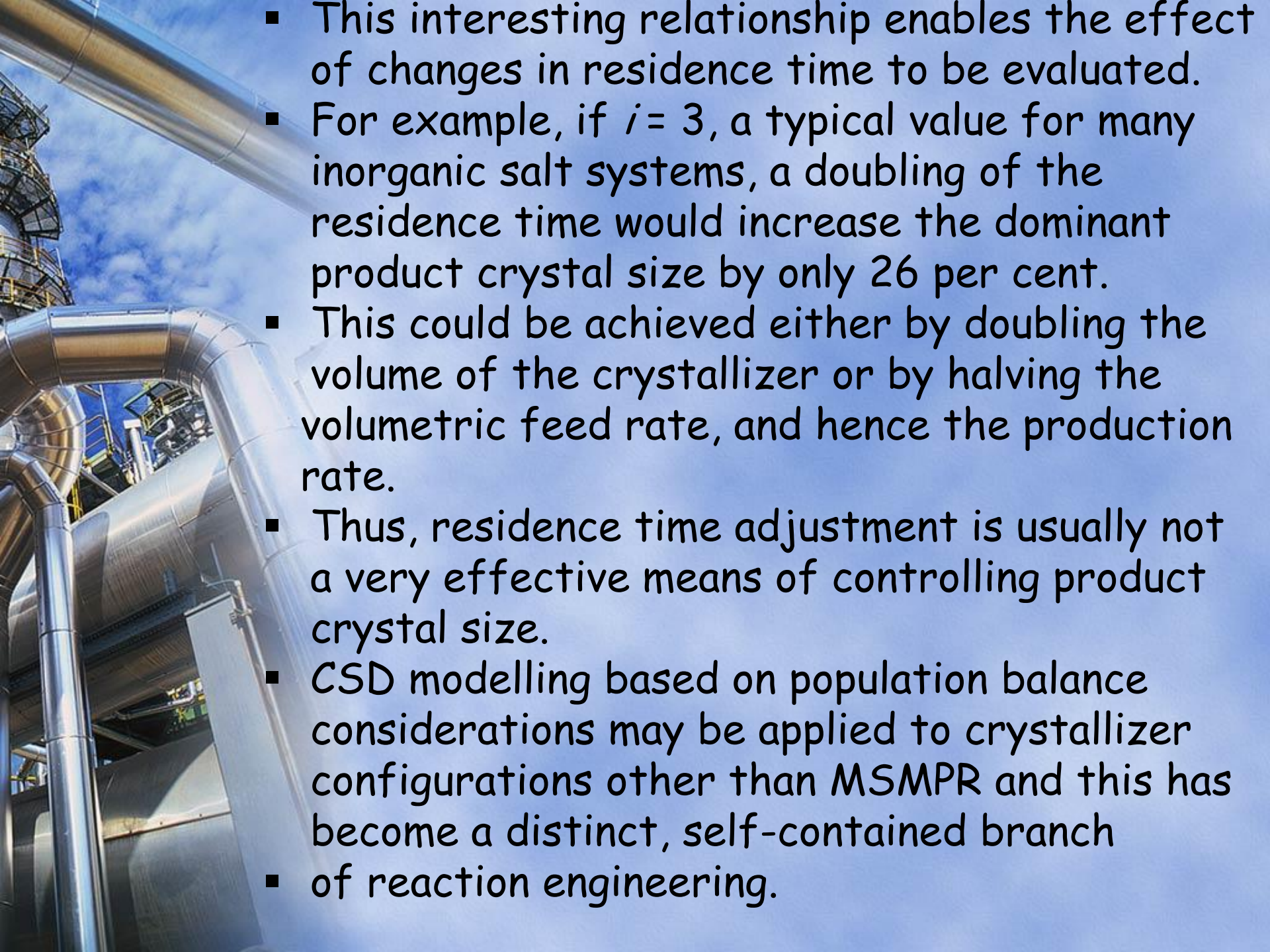
where α is the volume shape factor defined by $\alpha = \text{volume}/d^3$ and ρ is the crystal density.

The peak of the mass distribution, the dominant size d_D of the CSD, is given by

$$d_D = 3 G_d t_r$$

and this can be related to the crystallisation kinetics by:


$$d_D \propto t_r^{(i-1)/(i+3)}$$




- This interesting relationship enables the effect of changes in residence time to be evaluated.
- For example, if $i = 3$, a typical value for many inorganic salt systems, a doubling of the residence time would increase the dominant product crystal size by only 26 per cent.
- This could be achieved either by doubling the volume of the crystallizer or by halving the volumetric feed rate, and hence the production rate.
- Thus, residence time adjustment is usually not a very effective means of controlling product crystal size.
- CSD modelling based on population balance considerations may be applied to crystallizer configurations other than MSMPR and this has become a distinct, self-contained branch
- of reaction engineering.

Η δομή της διεπιφάνειας

- Η επιφανειακή τραχύτητα (σε μοριακό επίπεδο) ποσοτικοποιείται με τη βοήθεια του συντελεστή α ($\alpha = \Delta H/RT$) ο οποίος καθορίζεται από τις δυνάμεις που ασκούνται στη διεπιφάνεια μεταξύ κρυστάλλου και του μέσου εντός του οποίου λαμβάνει χώρα η κρυστάλλωση.
- Μεταβολές του συντελεστή α είναι δυνατόν να επηρρέασουν την δυναμική της ανάπτυξης μιας έδρας και ως εκ τούτου το σχήμα του κρυστάλλου.
- Σε πολλές περιπτώσεις, η αλλαγή του διαλύτη έχει ως αποτέλεσμα την αλλαγή της μορφοτροπίας των κρυστάλλων. Η αλλαγή αυτή μπορεί να ερμηνευτεί βάσει των μεταβολών στη δομή της διεπιφάνειας.

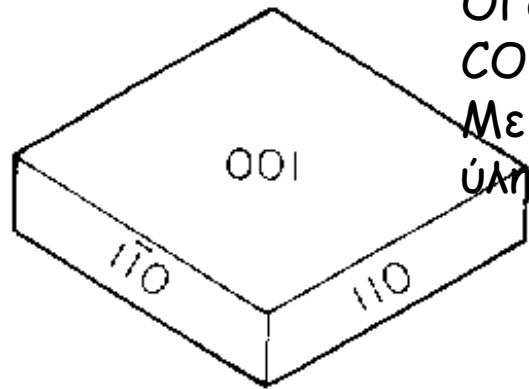
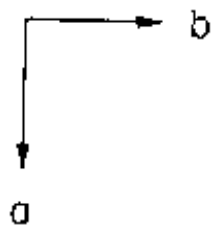
- 
- A photograph of industrial machinery, including large metal pipes and a complex structure, likely part of a refinery or chemical plant. The image is partially obscured by a white text box.
- Όσο μεγαλύτερη είναι η διαλυτότητα μιας ουσίας σε ένα διαλύτη, τόσο μικρότερη είναι η αντίστοιχη τιμή του συντελεστή α
 - Η επιφάνεια γίνεται περισσότερο τραχεία.
 - Έδρες F (μεγάλες τιμές του α) ευνοούν τον μηχανισμό κρυσταλλικής ανάπτυξης BCF (ανάπτυξη σε ελικοειδείς εξαρθρώσεις)
 - Όσο τραχύτερη μια επιφάνεια (χαμηλές τιμές α) μηχανισμός επιφανειακής διάχυσης
 - Ενδιάμεσες τιμές τραχύτητας, μηχανισμός γέννησης-εξάπλωσης (Birth and Spread (B+S)).



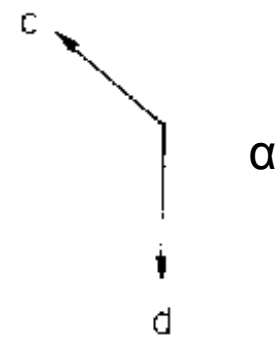
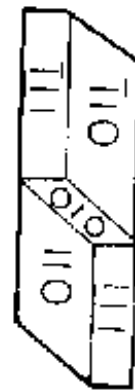
❖ Οι μηχανισμοί, χαρακτηρίζονται από διαφορές της εξάρτησης του ρυθμού κρυσταλλικής ανάπτυξης από τον υπερκορεσμό οπότε αναμένεται:

❖ Διαφορετικές κρυσταλλικές έδρες αναπτύσσονται με διαφορετικούς ρυθμούς σε διαφορετικούς διαλύτες με αποτέλεσμα να προκύπτουν διαφορετικές μορφοτροπίες για τους ίδιους κρυστάλλους

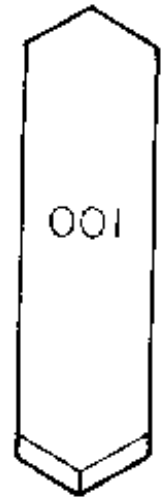
❖ Habit Modification of Succinic Acid Crystals Grown from Different Solvents, *Journal of Crystal Growth* 58(1982), 304-312.



Οι ομάδες -COOH κάθετες
Μείωση ροής
ύλης με διάχυση



Οι συντελεστές α παρόμοιοι άρα οι όποιες μεταβολές στη μορφοτροπία οφείλονται στην αλληλεπίδραση με το διαλύτη

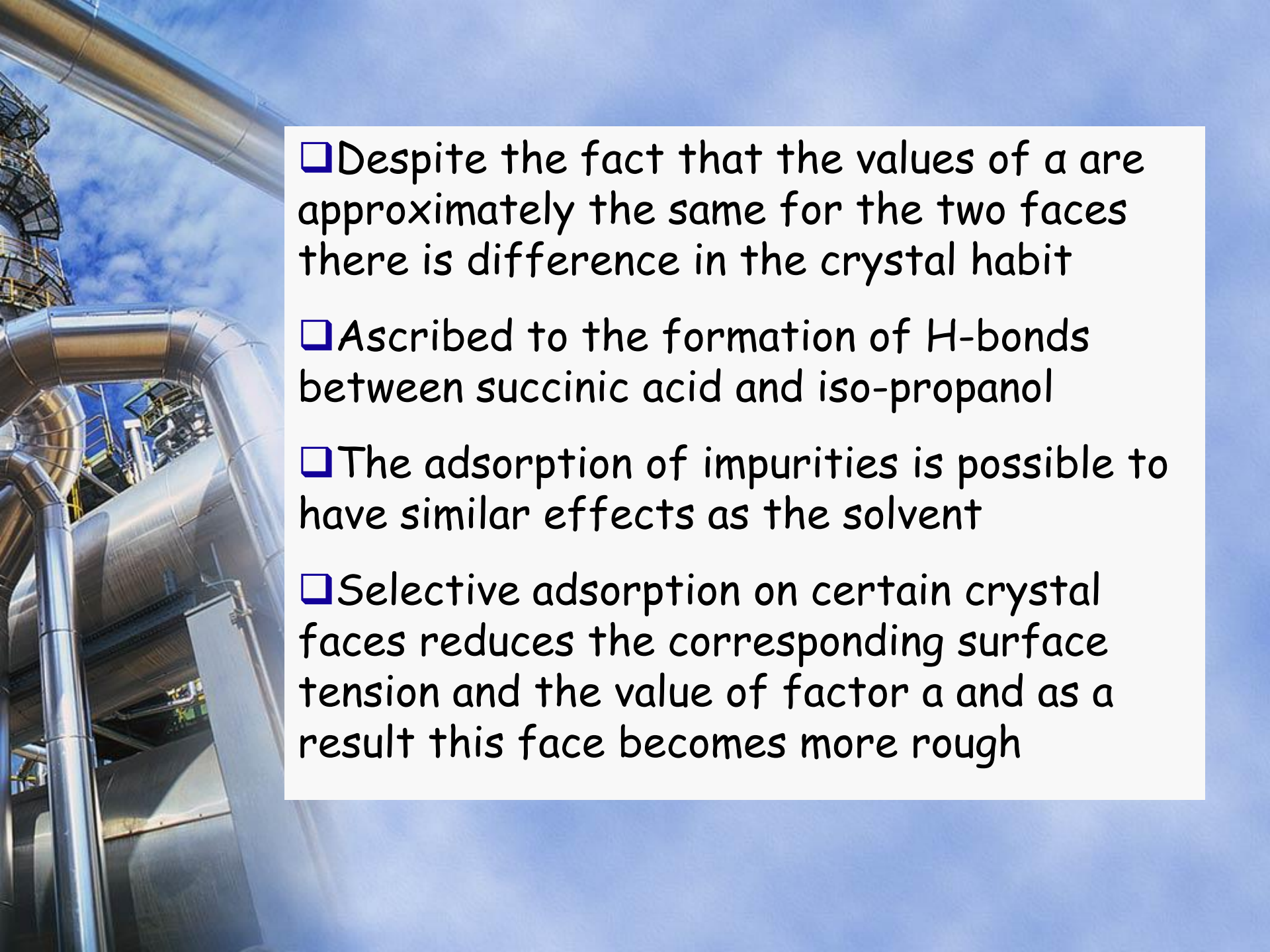


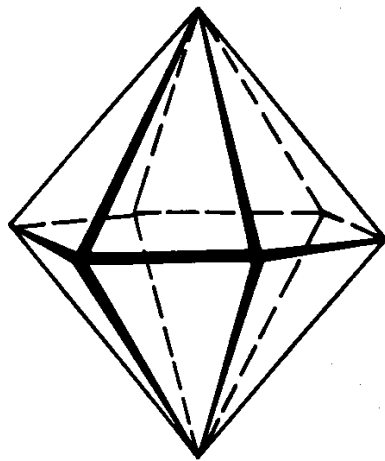
Ισχυρότερη αλληλεπίδραση ΗΟ με ΙΠ λόγω δεσμών υδρογόνου



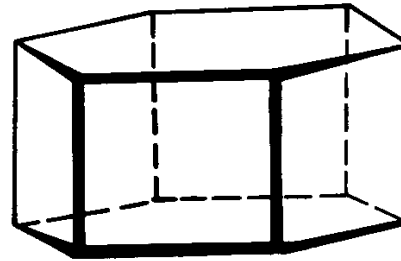
β
-COOH στις (010) παράλληλες αποτελεσματική ρόφηση

Ηλεκτρικό οξύ (succinic acid) α: crystallized in water β: in iso-propanol (Davey, Whiting, Mullin, 1982).

- 
- A photograph of an industrial facility, likely a refinery or chemical plant, featuring large, shiny metal pipes and structures against a clear blue sky. The pipes are arranged in a complex network, with some curving upwards and others running horizontally. The background shows a bright blue sky with a few wispy clouds.
- ❑ Despite the fact that the values of α are approximately the same for the two faces there is difference in the crystal habit
 - ❑ Ascribed to the formation of H-bonds between succinic acid and iso-propanol
 - ❑ The adsorption of impurities is possible to have similar effects as the solvent
 - ❑ Selective adsorption on certain crystal faces reduces the corresponding surface tension and the value of factor α and as a result this face becomes more rough

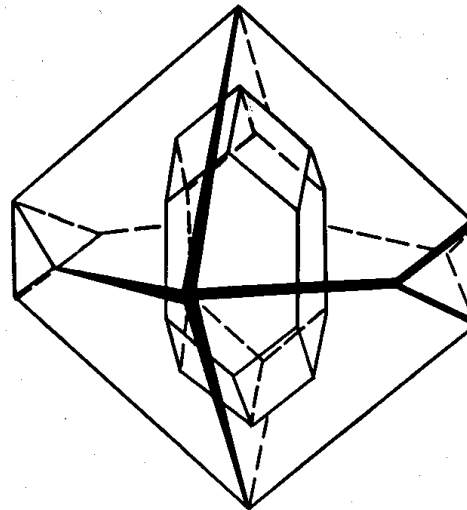


(a)

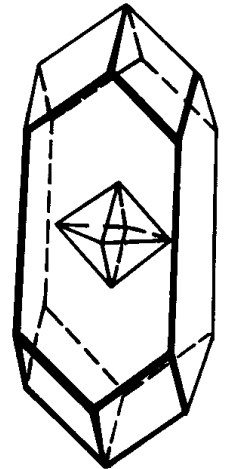


(b)

Fig. 5-13. Variation of the crystal habit of iodoform when grown from (a) aniline and (b) cyclohexane. (After Wells, ref. 38)



(a)



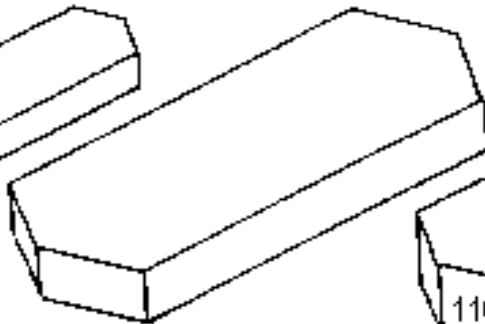
(b)

Fig. 5-14. Variation of the crystal habit of anthranilic acid grown from (a) ethanol and (b) glacial acetic acid. (After Wells, ref. 38)

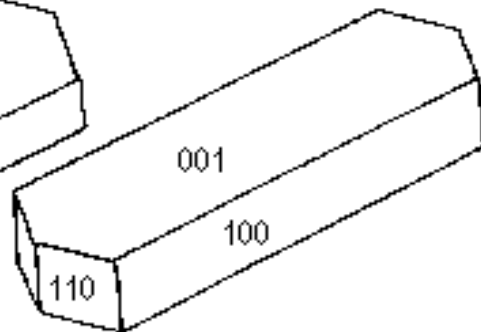
Σχήμα Κρυστάλλου- π.χ. ibuprofen



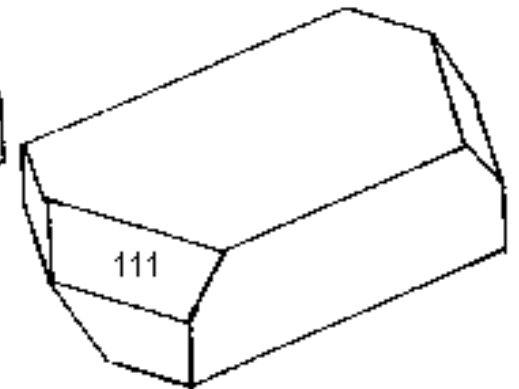
hexane



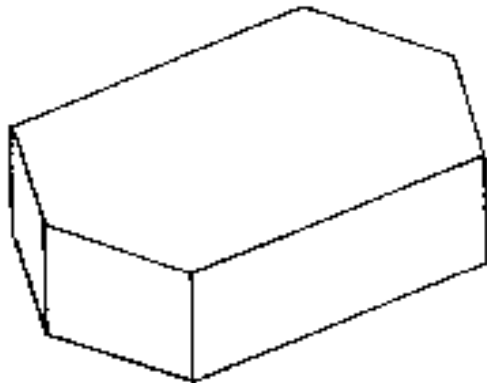
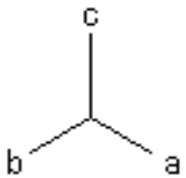
toluene



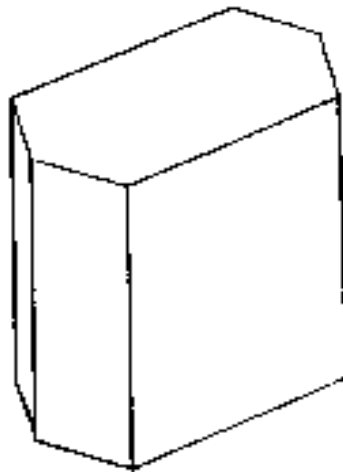
ethyl acetate



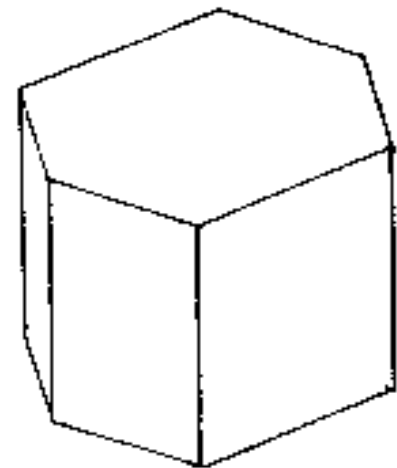
acetonitrile



propan-2-ol

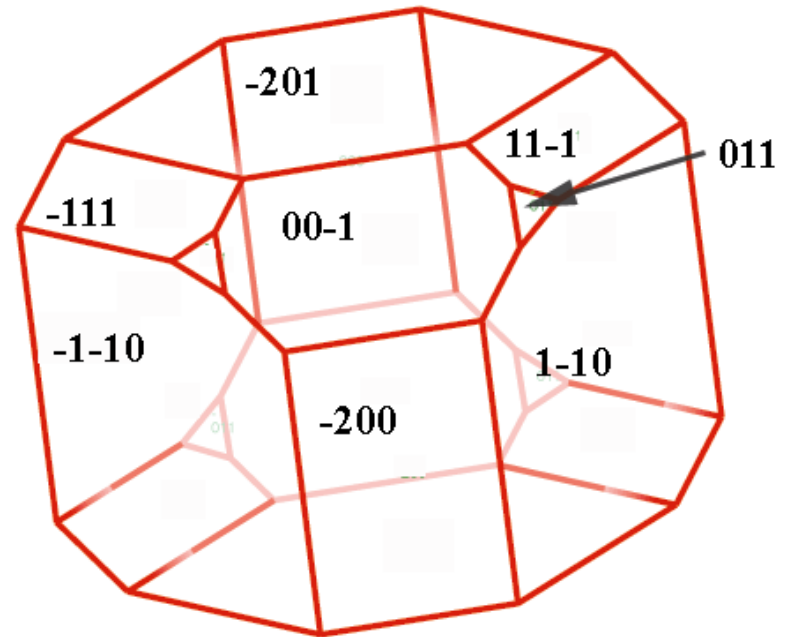
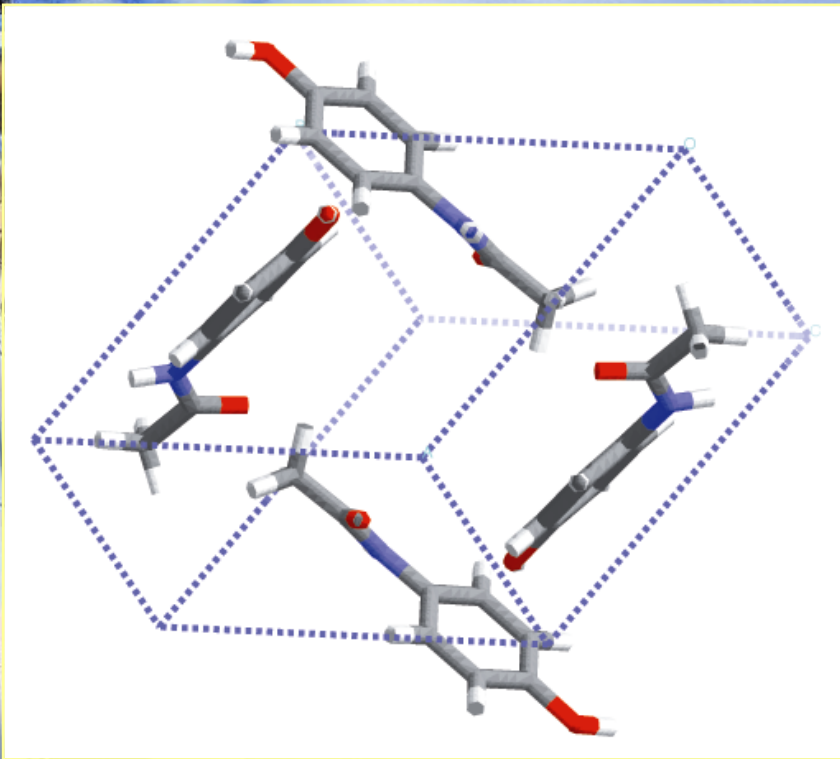


ethanol

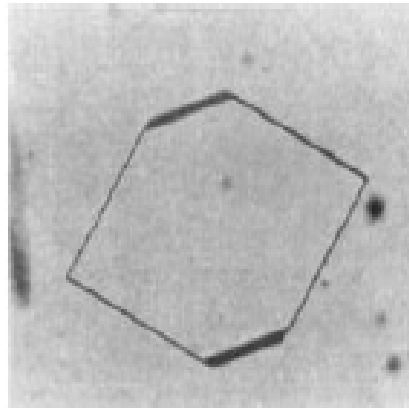


methanol

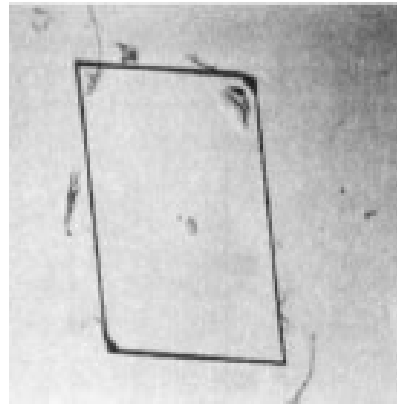
Paracetamol – έδρες



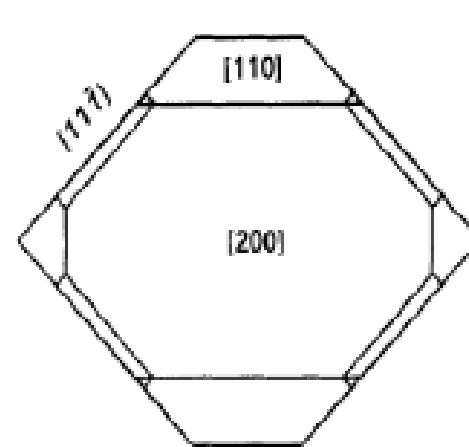
Μοναδιαία
κυψελίδα



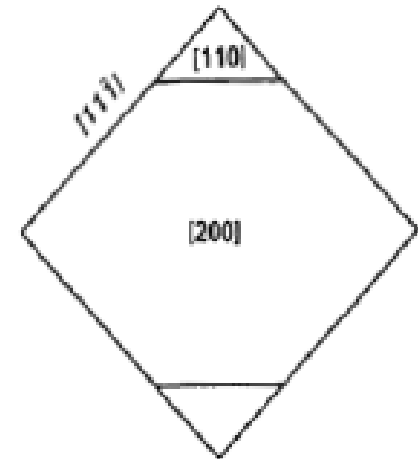
a



b



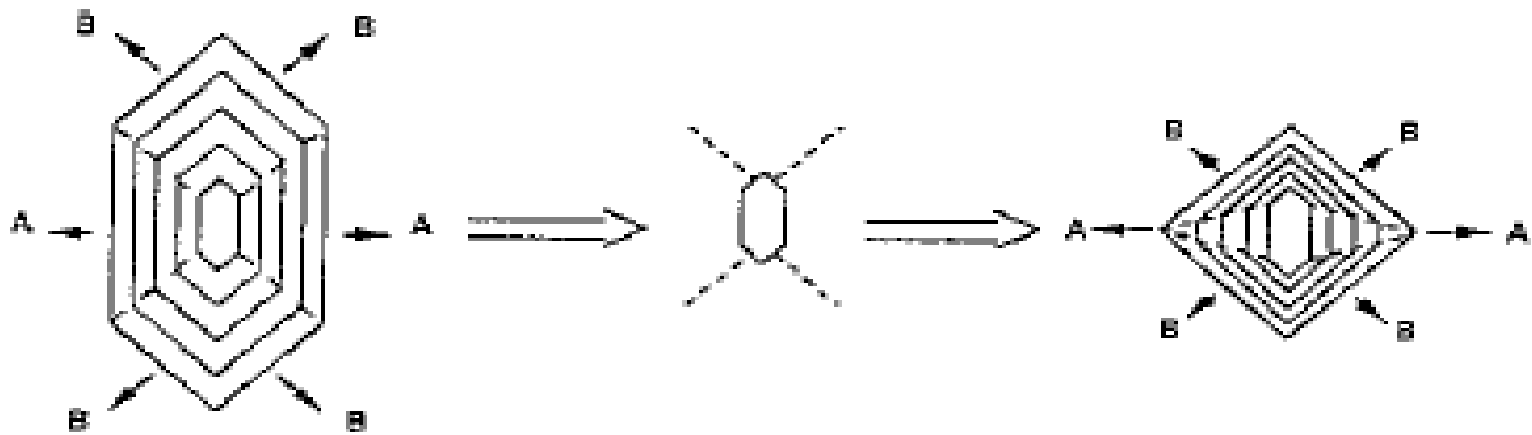
c



d

Figure 28. Images of caprolactam morphologies. a) pure caprolactam grown from the melt, b) caprolactam in the presence of 5% ethanol, c) the theoretical pure caprolactam morphology and d) the predicted morphology grown in the presence of ethanol. Image taken from "Designing Crustal Morphology by a Simple Approach"⁶⁴.

- ❖ Crystal habit is determined from the relative rate of growth in the various directions
- ❖ The faster the growth to a certain direction the respective face (perpendicular to this direction) the **smaller** it shall be
- ❖ If therefore growth towards a certain direction, perpendicular to a crystal face, is inhibited the respective surface is expected to increase in comparison with the rest of the crystal faces

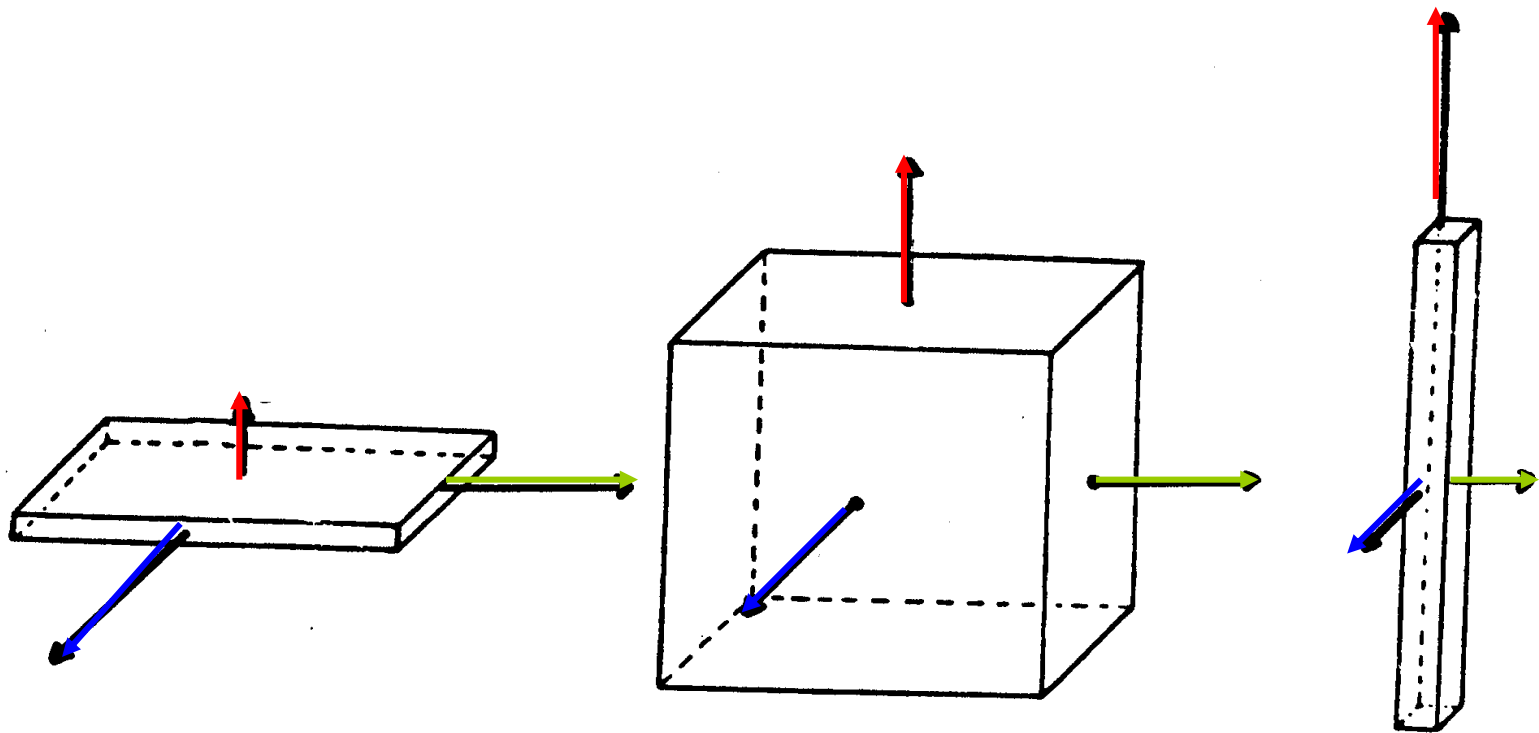


Unaffected crystal growth
rate of growth $B \approx A$

Stereoselective adsorption
of additive inhibits the
growth of the B faces

Affected crystal growth
rate of growth $A < B$

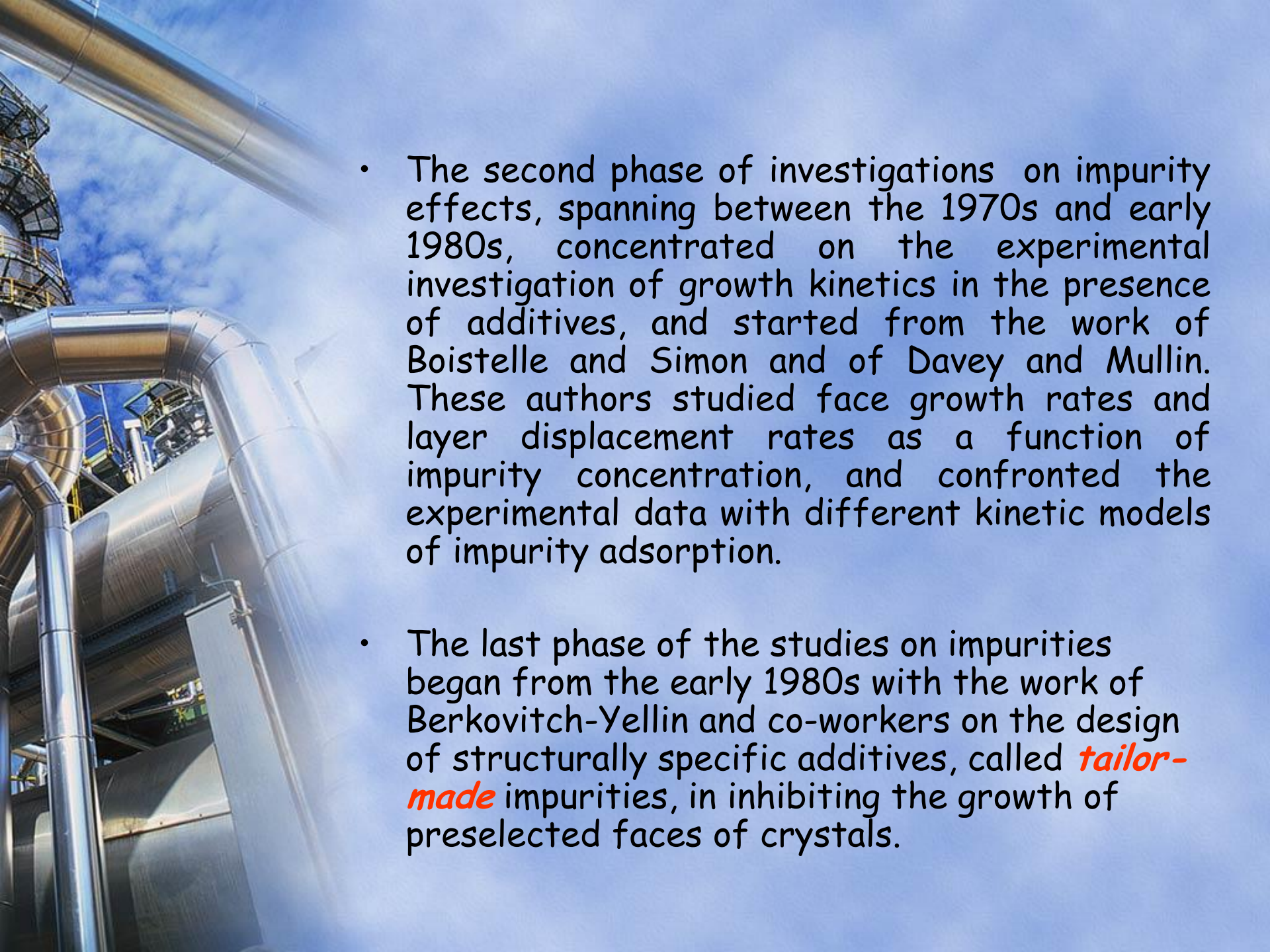
Σχήμα κρυστάλλων



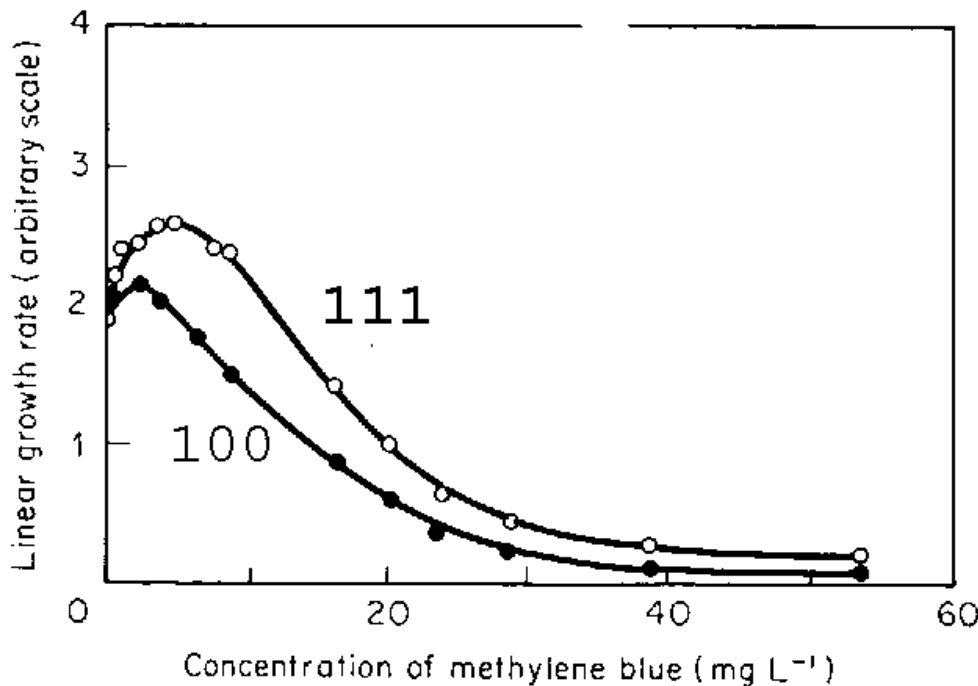
(a)

Additives(Επιμολύνσεις) and Crystal Habit

- The literature existing prior to 1950 on the habit modification of crystals by impurities has been surveyed in the **classical monograph** by Buckley [**Crystal Growth, John Wiley & Sons, New York (1951)**].
- After the publication of this monograph, efforts were diverted to understanding the basic mechanisms responsible for changes in the growth habit of crystals caused by impurities on the microscopic level.
- The first important work in this direction was published during the late 1950s and 1960s when kinetic models describing the motion of ledges across the surface of a crystal were formulated theoretically in terms of adsorption of impurity particles at surface terrace (Cabrera-Vermilyea model), ledges (Sears model) and kinks (Bliznakov model). During this period, on the basis of their experimental results on the growth forms of alkali metal halides as a function of supersaturation and impurity concentration, Kern and his associates advanced the structural interpretation of habit modification in terms of the formation of two-dimensional adsorbed-impurity layers similar to epitaxial relationships in epitaxial growth.

- 
- The second phase of investigations on impurity effects, spanning between the 1970s and early 1980s, concentrated on the experimental investigation of growth kinetics in the presence of additives, and started from the work of Boistelle and Simon and of Davey and Mullin. These authors studied face growth rates and layer displacement rates as a function of impurity concentration, and confronted the experimental data with different kinetic models of impurity adsorption.
 - The last phase of the studies on impurities began from the early 1980s with the work of Berkovitch-Yellin and co-workers on the design of structurally specific additives, called *tailor-made* impurities, in inhibiting the growth of preselected faces of crystals.

Impurities may have dual action: Accelerating or Retarding



The influence of methylene blue on the (100) and (111) face growth rates of lead nitrate at 25°C and $S = 1.08$, showing a reversal of effect. (After Bliznakov, 1965)

The background of the slide is a photograph of an industrial facility, likely a refinery or chemical plant. It features several large, shiny, metallic pipes that curve and connect various pieces of equipment. The sky is a clear, bright blue with some light, wispy clouds. The overall scene is brightly lit, suggesting a sunny day.

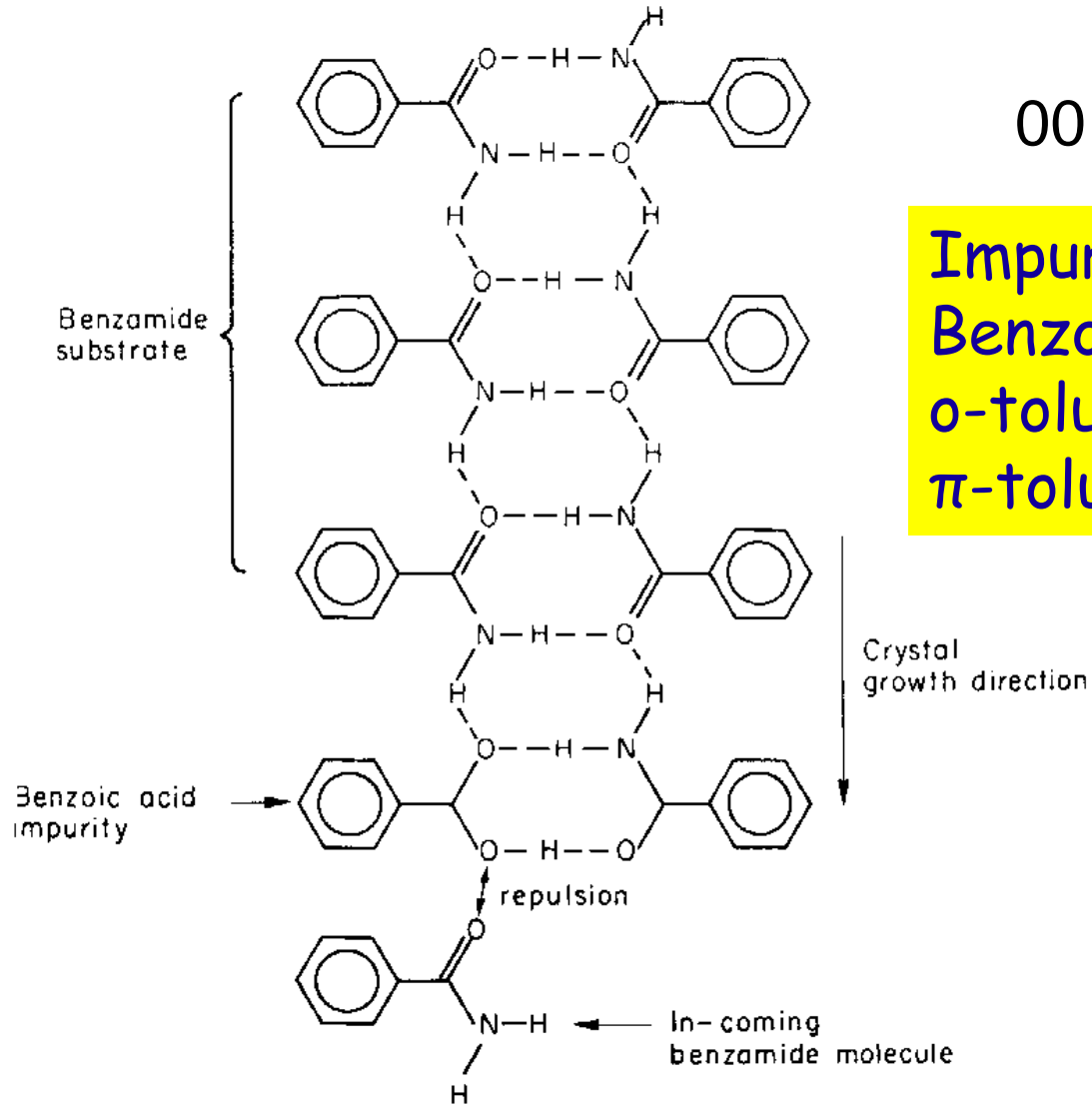
Structural compatibility

- Structural compatibility between «impurity» and crystal growing substance
- Tailored (κατά παραγγελία) crystal growth
- Impurities of this type have two types of functional groups: one compatible with a crystal face (affinity-grafting) and the other is repelled



001

Impurities:
Benzoic acid,
o-toluamide,
 π -toluamide



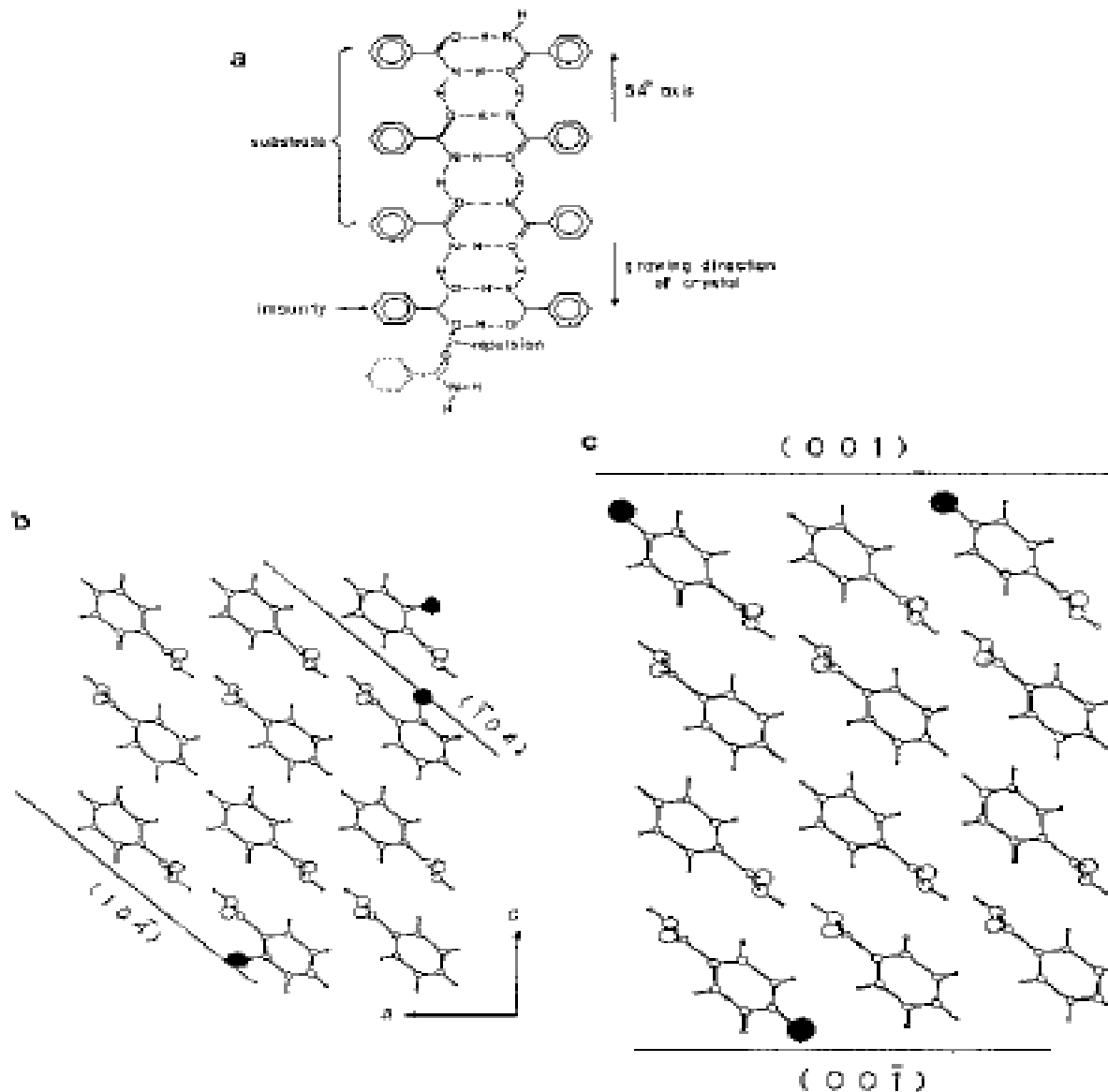


Figure 2.4. (a) Schematic representation of the ribbon motif of hydrogen-bonded dimers of benzamide molecules interlinked along the 5-Å b axis; (b) packing arrangement of benzamide, viewed along the b axis, showing the effect of o -toluamide inhibiting growth along the a direction; (c) packing arrangement of benzamide, viewed along the b axis, showing the effect of p -toluamide inhibiting growth along the c direction.

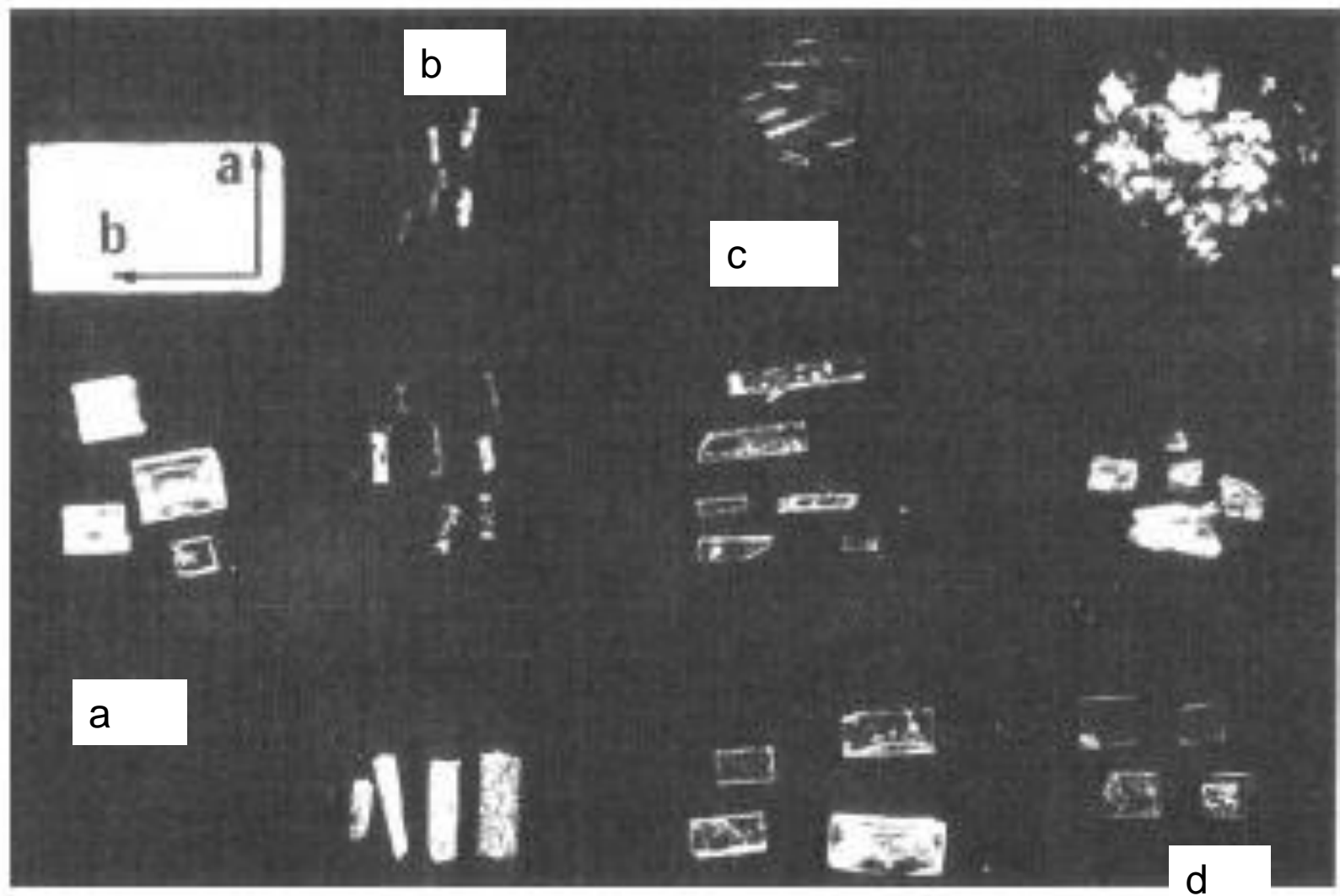


Figure 2.5. Crystals of benzamide: (a) pure and (b) (d) grown in the presence of additives: (b) benzoic acid; (c) *o*-toluamide; (d) *p*-toluamide.

Η σημασία της μορφοτροπίας (Habit) στη βιομηχανία

Στην περίπτωση κρυστάλλων που προορίζονται για εμπορική χρήση, υπάρχουν μορφοτροπίες που είναι ανεπιθύμητες λόγω της ανεπιθύμητης εμφάνισης την οποία προσδίδουν στο μακροσκοπικό υλικό ή προκαλούν δυσκολίες στη συσκευασία ή στη διαχείριση.

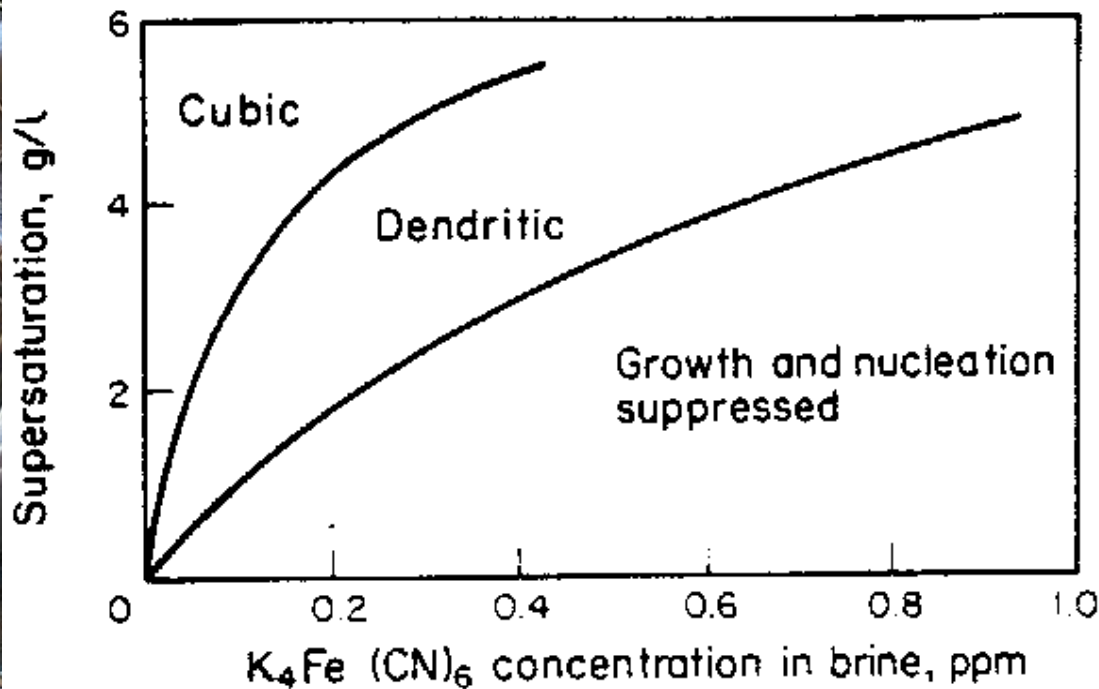
Η εμπορικά επιθυμητή μορφοτροπία είναι συνήθως η κοκκώδης και η πρισματική, χωρίς να αποκλείονται και άλλα είδη (πλακοειδείς, βελονοειδείς). Διάφορα είδη συνοψίζονται στον πίνακα ο οποίος ακολουθεί.

Σε κάθε διεργασία παραγωγής κρυσταλλικών υλικών, υπάρχουν διεργασίες ελέγχου ή κατεύθυνσης της μορφοτροπίας. Οι διεργασίες αυτές συνίστανται στον έλεγχο του υπερκορεσμού, του ρυθμού ψύξης ή εξάτμισης, ή της θερμοκρασίας, ή στην επιλογή του κατάλληλου διαλύτη, ρύθμιση του pH σε συγκεκριμένη τιμή ή και στην προσθήκη ορισμένης συγκέντρωσης επιμόλυνσης, ή συνδυασμοί των παραπάνω



<i>Substance</i>	<i>Normal habit</i>	<i>Habit modifier</i>	<i>Changed habit</i>
NH ₄ alum	octahedra	borax	cubes
NH ₄ Cl	dendrites	Cd ²⁺ , Ni ²⁺	cubes
NH ₄ H ₂ PO ₄	needles	MnCl ₂ + HCl	granules
NH ₄ NO ₃	squat crystals	Al ³⁺ , Fe ³⁺ , Cr ³⁺	tapered prisms
(NH ₄) ₂ SO ₄	prisms	Acid Magenta	needles
H ₃ BO ₃	needles	Fe ³⁺	irregular crystals
CaCO ₃		H ₂ SO ₄	needles
CaSO ₄ · 2H ₂ O	needles	gelatin, casein	flakes
		alkyl aryl	
		sulphonates	granular precipitate
		sodium citrate	prisms
		alkyl aryl	
		sulphonates	prisms
MgSO ₄ · 7H ₂ O	needles	borax	prisms
AgNO ₃	plates	sodium oleate	dendrites
K alum	octahedra	borax	cubes
KBr	cubes	phenol	octahedra
KCN	cubes	Fe ³⁺	dendrites
KCl	cubes	Fe(CN) ₆ ⁴⁻	dendrites
		PbCl ₂	octahedra
K ₂ SO ₄	rhombic prisms	Fe ³⁺	irregular needles
NaBr	cubes	Fe(CN) ₆ ⁴⁻	dendrites
NaCN	cubes	Fe ³⁺	dendrites
NaCl	cubes	Fe(CN) ₆ ⁴⁻	dendrites
		formamide	octahedra
		Pb ²⁺ , Cd ²⁺	large crystals
		polyvinylalcohol	needles
		Na ₆ P ₄ O ₁₃	octahedra
Na ₂ B ₄ O ₇ · 10H ₂ O	elongated prisms	NaOH, Na ₂ CO ₃	squat prisms
		carboxy methyl	flakes
		cellulose	
NaClO ₃	cubes	S ₂ O ₆ ²⁻	octahedra
PbCl ₂	plates	dextrin	bisphenoids
Sucrose	prisms	raffinose	needles

Σε περίπτωση κατά την οποία η μορφοτροπία των σχηματιζόμενων κρυστάλλων εξαρτάται από περισσότερους του ενός παράγοντες (π.χ. υπερκορεσμός και παρουσία επιμολύνσεων) το αποτέλεσμα του συνδυασμού αυτού αποτυπώνεται στα Morphograms (Μορφολογικά διαγράμματα)



Morphogram for the crystallization of sodium chloride from the system $K_4Fe(CN)_6-NaCl-H_2O$ at $42^\circ C$.

The effect of impurities on crystal habit

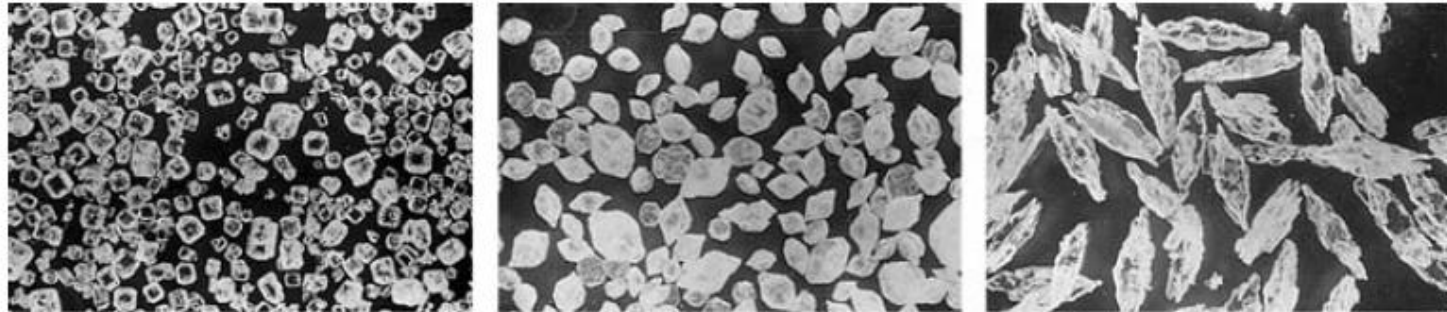


Figure 6.40. *Habit changes in ammonium sulphate crystals caused by traces of impurity: (a) pure solution, (b) 5 ppm Cr³⁺, (c) 20 ppm Cr³⁺. (Larson and Mullin, 1973)*



Figure 6.41. *Habit changes in sodium chloride crystals caused by traces of impurity: (a) pure solution, (b) 0.1% Fe(CN)₆⁴⁻, (c) 1% Fe(CN)₆⁴⁻. (Cooke, 1966)*

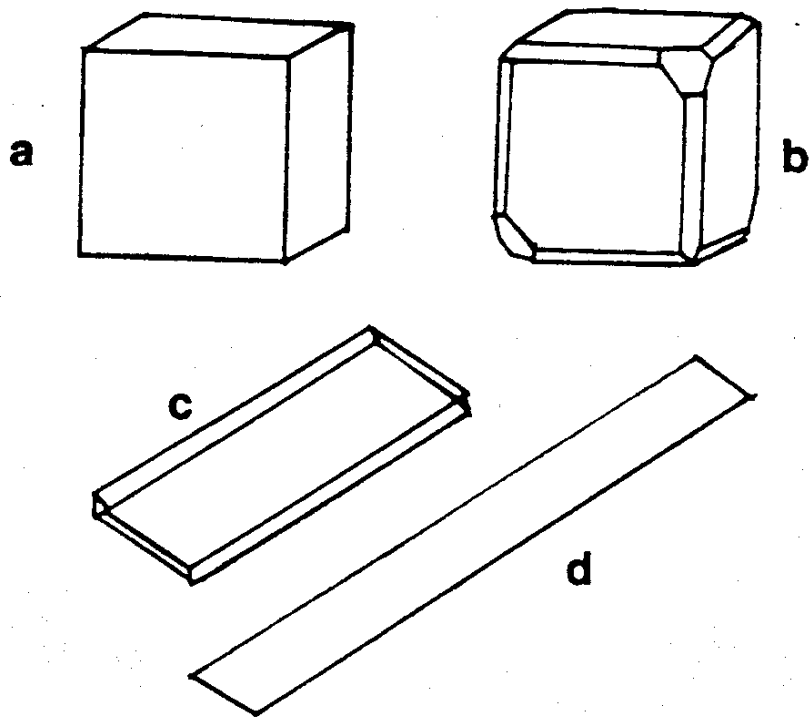


Figure 2.16 Variation of crystal shape with conditions of growth. Sodium chlorate grown (a) rapidly and (b) slowly. Gypsum grown (c) slowly and (d) rapidly. (Reproduced with permission from Bunn 1961.)

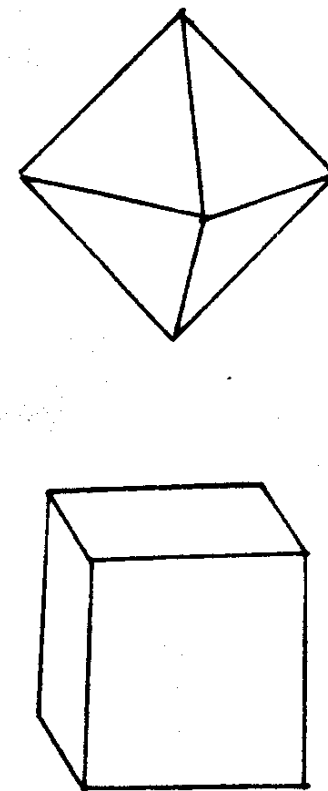


Figure 2.18 Sodium chloride crystals grown from pure solution and from a solution containing 10% urea. (Reproduced with permission from Bunn 1961.)

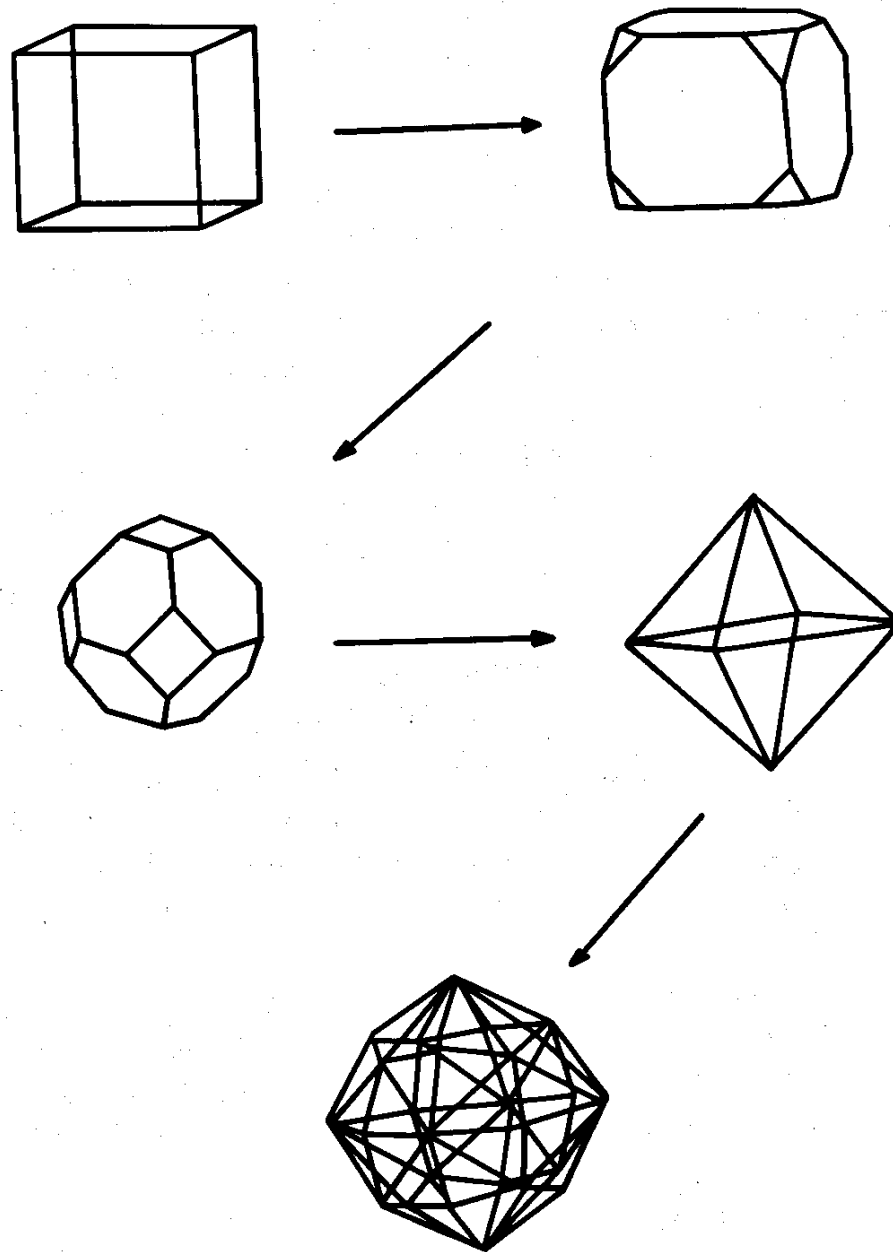


Fig. 5-15. Some possible modifications of a cubic system showing formation of the octahedral faces, then higher-index faces.